# Sea Level Variability and Coastal Trapped Waves around southern Africa

**Bernardino João Nhantumbo**



Dissertation presented in partial fulfillment of the requirements for the degree of Master of Science in Ocean and Climate Dynamics

Department of Oceanography

UNIVERSITY OF CAPE TOWN
IYUNIVESITHI YASEKAPA • UNIVERSITEIT VAN KAAPSTAD

Supervisor: Prof. Frank Shillington

February 2014

## ABSTRACT

The propagation characteristics of the coastal trapped waves (CTWs) around the coast of southern Africa were investigated by analyzing the observed daily mean sea level data from 16 coastal tide gauges, as well as outputs of sea level anomalies from the Hybrid Coordinate Ocean Model (HYCOM) at a grid point closest to each tide gauge station under consideration. The observed records showed sea level variability dominated by the short time variability with a period shorter than one month. This short time variability varies from season to season with the largest CTW amplitude during austral winter. The short time variability propagates anticlockwise as coastal trapped wave around the coast of southern Africa with a propagation speed ranging from 3 to 6.5 m/s, and from 1 to 7.5 m/s, along the west and south coasts, respectively. These propagation speeds are forced by synoptic atmospheric disturbances mainly in term of wind variability. Coastal trapped waves were observed propagating equatorward in the east coast of southern Africa in the opposite direction of Agulhas current on a few occasions. It can be a result of a good resonance between a strong and persistence of weather system and the coastal trapped wave. It is believed that more precise response and good answers for some discrepancies that were found can be achieved when a longer time records from Inhambane is included in future similar study. The outputs from HYCOM showed very similar propagation characteristics to the observed data. Along the south coast, the behaviour of the CTW is well reproduced. Unfortunately the model does not reproduce very well the variability along the west coast. While it seems to underestimate the west coast response, at same time it seems to overestimate it along the south coast of southern Africa. Although the model demonstrated some CTWs travelling northwards along the east coast, such disturbances were infrequent and difficult to find in the observed data.

# Contents

## Declaration

"I know the meaning of Plagiarism and declare that all of the work in the document, save for that which is properly acknowledged, is my own"

Signature: Signed by candidate
Signature removed

Date: 14/02/2014

## Acknowledgments

I thank to the NANSEN - TUTU CENTRE for Marine Environmental Research for providing an incommensurable help by fully sponsoring my MSc studies. I would like to express my sincere thanks to Dr. Atanásio Manhique, Prof. Alberto Mavume and Prof. Chris Reason, the key persons for my presence in the Department, to continue with my studying advancement. I also would like to thank my employer, National Institute of Meteorology – Mozambique (INAM) for the permission to attend this master program in order to get and improve research skills for our Department of Research.

I am particularly indebted to my excellent supervisor, Prof. Frank Shillington, for a very good "networkness" between me and him. His office's door was always open for me to provide support, inspiration, guidance and encouragement. His explanations and questions produced strength, confidence and improvement in my understanding of the thesis and also to my English. I also thank to Prof. Chris Reason for suggestions of relevant resource materials to understand my thesis topic.

To Julie, Bjorn, Vincent, Issufo and Yonss, my tutors of MATLAB©, my warm thanks. My special thanks to Julie Deshayes for helping with the spectral analysis and Bjorn Backeberg for providing the HYCOM numerical model outputs. I also thank my compatriots at University of Cape Town for their encouragement throughout the course.

I am grateful for sharing the same place with a "dream time", Lerato, Lebo, Daneeja, Laura, Precious, Mthetho, Xolisa, Fehmi and Chris, my fellows Ocean and Climate dynamics 2013. I had also a very interesting relationship with, both co-students and scientists in the Department, for which I am also grateful.

Finally, my thanks to Celeste, my wife, my partner, my friend; has been my rock throughout this journey. I left her with a challenge to take care our daughters (Tiana and Mari) and managing our home with very limited financial resources, she did not disappoint me. I thank mum (the best mum in the world), my family and friends for their support. I thank God for blessing me with this opportunity, and helping and supporting me throughout my paths.

## List of Figures

## List of Tables

**Acronyms**

| | |
|---|---|
| CTW | Coastal Trapped Wave |
| HYCOM | Hybrid Coordinate Ocean Model |
| IOC | Intergovernmental oceanographic commission |
| MSL | Mean Sea Level |
| NTDE | National Tidal Datum Epoch |
| NOAA | National Oceanic and Atmospheric Administration |
| CKW | Coastal Kelvin Wave |
| CSW | Continental Shelf Wave |
| OGCM | Ocean General Circulation Model |
| ITCZ | Inter-tropical Convergence Zone |
| UHSLC | University of Hawaii Sea Level Centre |
| NCAR | National Centre for Atmospheric Research |
| CIRES | Cooperative Institute for Research in Environmental Sciences |
| NCEP | National Centre for Environmental Prediction |
| SLA | Sea Level Anomaly |
| SLP | Sea Level Pressure |
| MATLAB© | MATrix LABoratory |
| INAM | National Institute of Meteorology – Mozambique |
| ECMWF | European Centre for Medium-Range Weather Forecast |

## List of Symbols

| | |
|---|---|
| $Z_t$ | Observed sea level height |
| $Z_0$ | Mean sea surface level component |
| $X_t$ | Gravitational tide component |
| $S_t$ | Meteorological residuals component |
| $L$ | Characteristic shelf-slope width |
| $cm$ | Centimetre |
| $x$ | Displacement perpendicular to the coast |
| $u$ | Offshore velocity component |
| $y$ | Displacement along the coast |
| $v$ | Alongshore velocity component |
| $H$ | Water depth variation |
| $D$ | Mean deep-sea depth far from the coast |
| $f$ | Coriolis frequency |
| $\eta$ | Magnitude of any type of surface disturbance (elevation) |
| $km$ | Kilometre |
| $\rho_0$ | Water density |
| $p$ | Water pressure perturbation |
| $t$ | Time |
| $g$ | Acceleration due to Earth's gravity |
| $z$ | Vertical Displacement (positive upwards) |
| $\rho$ | Water density perturbation |
| $w$ | Vertical velocity component |
| $\bar{\rho}$ | Mean water density |
| $N$ | Buoyancy frequency |
| $h$ | Local depth of the ocean |
| $F_n$ | Across-shore modal solution |
| $n$ | Number of modes |
| $l_n$ | Real positive alongshore wave-number |

| | |
|---|---|
| $\omega$ | Complex frequency |
| $C_n$ | Phase speed |
| $mm$ | Millimetre |
| $m$ | Metre |
| $s$ | Second |
| $\dot{y}$ | Interpolated value |
| $\dot{x}$ | Time or position of the desired interpolated value |
| $a$ | Times or positions of the data collection at the start of the sampling increment being interpolated |
| $b$ | Times or positions of the data collection at the end of the sampling increment being interpolated |
| $Z$ | Adjusted sea level height |
| $\overline{AP}$ | Mean surface pressure |
| $AP$ | Actual surface pressure |
| $mb$ | Milli-bar |
| $Pa$ | Pascal |

# CHAPTER 1

# INTRODUCTION

## 1.1 General

Coastal Trapped Waves (CTWs) forced by the wind stress, actually the alongshore component of wind stress (Robinson, 1964; Mysak, 1967; Adams and Buchwald, 1969; Gill and Schumann, 1974; LeBlond and Mysak, 1978), are the object of study in this work. One of the best ways to observe CTW's, is to start by analyzing the behaviour of the sea level on the continental shelf. The variations in sea level measured at coastal sites can bring evidence of occurrence of the CTWs along the world's coastlines. In order to achieve this, it is best to plot sea level records from different tide gauges that are closely spaced along the shelf. This is likely to reveal patterns of low frequency (days) sea level variability.

The CTWs were intensely studied in the 1980s (Reynaud et al., 1991) and these studies revealed that they propagate towards the equator on the west boundary of the oceans and towards the poles on the east boundary of the oceans; have periods of days to weeks, and are mainly driven by alongshore wind fluctuations. These CTWs are a mechanism by which winds at one location are able to influence the coastal ocean in other locations at large distances.

Thus, the existence of those waves has been revealed in many ocean boundaries around the world (LeBlond and Mysak; 1978; Mysak, 1980; Reynaud et al., 1991). Around the coast of southern Africa, de Cuevas et al. (1986) concluded that the sea level disturbances that they found propagating down the west coast and along the south coast are coastal trapped waves. They concluded also that those disturbances did not continue propagating northwards along the east coast, north of Durban. Schumann and Brink (1990) confirmed the existence of coastal trapped waves by studying their propagation characteristics. Their results suggest that

the CTWs are inhibited by the Agulhas Current, as was previously reported by de Cuevas et al. (1986), on their eastward and equatorward propagation. Brink (1990) reported results similar to this latter finding. The effect of the Agulhas Current on the propagation of CTWs was first speculated by Gill and Schumann (1979). The studies carried by de Cuevas et al. (1986) and, Schumann and Brink (1990) suggested the weather systems as the forcing mechanisms to establish the existence of coastal trapped waves. But more than establish, the CTWs must be continually forced to propagate, with their speed determined by the speed of the forcing mechanism, around the coast of southern Africa (de Cuevas et al., 1986).

Therefore, an exercise to understand the relation between sea level variability and weather systems is necessary. The coastal sea level is affected by atmospheric pressure and wind disturbances in the coastal region as well as large-scale offshore forcing. This is the "isostatic" response, described by Robinson (1964). This direct response to air pressure is very rapid, and it can be shown that winds in the coastal region are the main forcing. The apparent "nonisostatic" sea level variability can be due to a sparse network of tide gauges which the results could easily be misinterpreted. This lack of direct response to local atmospheric pressure forcing could means that efforts must be given just to understand the action of the wind on the sea level variability. In this way the inverted barometric correction is applied just to reduce the ''noise'' related to regional phenomena in the tide gauge data (Church et al., 2004). The inverted barometric correction is an exercise usually made for adjusting coastal records assuming that 1 hPa increase (decrease) in the atmospheric pressure corresponds to 1 cm decrease (increase) in the sea level (Hamon, 1966; Buchwald and Adams, 1968; Mysak, 1967; Pugh, 1987; Schumann and Brink, 1990; Maiwa et al., 2009; Antunes and Taborda, 2009; Antunes, 2011).

In this study, sea level records were used to investigate sea level variations in order to identify coastal trapped waves around the coast of southern Africa. Later, the propagation of the forcing mechanism responsible for the sea level disturbances is also investigated to understand the propagation characteristics of CTWs along the east coast of southern Africa. The east coast of southern Africa is characterized by the activity of the western boundary current and the shelf is relatively narrow. These two facts are sufficient enough to inhibit the

normal existence and occurrence of CTWs along the aforementioned area where they were poorly investigated.

So, power spectrum density was used to detect frequency bands of significant energy peaks within the time series. The dominant modes of variability within the time series were detected using the wavelet power spectrum. By analyzing the Hovmöller diagrams, the propagation characteristics of the sea level variability were identified. The sea level heights from the Hybrid Coordinate Ocean Model (HYCOM) were used to understand if the model can reproduce signals with coastal trapped waves (CTWs) characteristics. It was possible by a comparison of both observed and model outputs sea levels pattern brought on the Hovmöller diagrams. The relationship between the sea level variability and the forcing agent is understood by interpreting the sequence of daily wind vectors and sea level pressure.

## 1.2 Problem Statement

The coastal trapped waves (CTWs) can have remarkable impacts on the marine bio-resources in the coastal and estuary regions. Therefore, the results of this study may be very important from both physical and biological aspects (Maiwa et al., 2009; Schuman, 2013). In addition, the question of coastal security is very important, taking into consideration that the countries located along the coast in the southern Africa have their major and most populous cities along the coast and/or along the borders of estuaries. As result of the coastal zone being densely populated when compared with other regions in the same countries, the question of sea level variability at all time scales needs to be addressed.

Rather than providing an exhaustive study of the subject of sea level variability, this study aims to improve the knowledge and so provide a better understanding of the CTWs at local and regional level around southern Africa. Since their discovery in 1960s (Hamon, 1962, 1966), CTWs have been the subject of many worldwide studies, with a concentration especially in the 1980s (LeBlond and Mysak, 1978; Mysak, 1980; Reynaud et al., 1991). Around the coast of southern Africa, few studies have been carried out, e.g. de Cuevas et al. (1986), Schumann and Brink (1990). These studies were focused on the existence and the

propagation characteristics of coastal trapped waves. Thus, the propagation characteristics of the CTWs are well known along the west and south region of the coast of southern Africa.

Therefore, although the behaviour of CTWs in the east region of the coast of southern Africa was already studied, e.g. Schumann (1983) and de Cuevas et al. (1986), there remain deficiencies (discrepancies) and open questions. An open question is whether CTWs are simply "stopped" from the travelling up the east coast, e.g. Gill and Schumann (1979), and will simply "die" near and around Richard's Bay, e.g. de Cuevas et al. (1986) or that they might continue northwards from Richard's Bay with renewed vigour in towards the equator (Shillington, pers. Comm.). There is a lack of adequate tide gauge records at Maputo or Inhambane, in Mozambique, and so possible CTW behaviour north of Richard's Bay is unknown. In addition to these unknowns, is the effect of the contribution of the coastal western boundary current; the very strong Agulhas Current, which propagates south-westwards in the opposite direction to the propagation of CTWs along the east coast of Africa, between Durban/Richards Bay and Port Elizabeth.

In addition to this, has been an interest in knowing the contribution of the CTWs to coastal nutrient transportation far away from the locations where the upwelling may occur. Rather than making an independent contribution, CTWs underlie and control circulation, exchange and mixing phenomena's in the coastal ocean. However, the performance of the CTWs on the nutrient transportation, for example, will depend on strength of the forcing mechanism (Huthnance, 1995).

It has been hypothesized that the combined effect of CTWS, together with severe storm surges due to say tropical cyclones along the east coast of Africa, large tides and possible tsunamis from the Indian Ocean may provide a dangerous, if rare, combination in this coastal region (Schuman, 2013).

Usually, the *in situ* observations have gaps, associated with problems faced by the institutions in managing tide gauges. Therefore outputs from the Hybrid Coordinate Ocean Model (HYCOM), for southern Africa, are used to reproduce the coastal trapped waves signal. If the signal is well reproduced, in future such outputs will be used to assess the occurrence of

CTWs around the coast of southern Africa. Taking into account what was before stated, key research questions were formulated.

## 1.3 Research questions

The aim of this study is to investigate the characteristics of daily sea level variability (amplitude, frequency, and speed of propagation) from tide gauges and to find characteristic patterns of the daily sea level variability from short term ocean numerical model outputs, around southern Africa, and later identify perturbations with CTWs characteristics. In order to reach this overall goal, two research questions are addressed:

i. Can the coastal trapped waves propagate equatorward along the east coast of southern Africa in the opposite direction of the Agulhas current?

ii. Can the HYCOM outputs of sea level anomalies, for southern Africa, reproduce the coastal trapped wave's signal of the tide gauges?

## 1.4 Structure of thesis

This thesis is organized into six chapters. Chapter 2 describes the nature of sea level variability and coastal trapped waves. It briefly explains factors contributing to sea level variability and differentiates "sea level" from "mean sea level", which helps to explain sea level variability. It also reviews the relevant studies which were undertaken to give scientific explanation of the existence of CTWs and describes the weather systems that rule the coast of southern Africa. Chapter 3 outlines the data used in the study and describes the research methodology. The results are presented in chapter 4. A discussion of the results is given in chapter 5. Chapter 6 provides the conclusions of this research.

There are also three technical appendices. Appendix A provides additional details relevant to assessment of frequency of coastal trapped waves in different sites around the coast of southern Africa. Appendix B brings auxiliary details relevant to assessment of propagation characteristics of coastal trapped waves in different sites around the coast of southern Africa.

Appendix C presents a sequence of daily wind vectors and sea level pressure around Southern Africa to provide additional details of the relation between the two variables during the generation and eastward propagation periods.

# CHAPTER 2

# LITERATURE REVIEW AND THEORY

## 2.1 Sea Level Variability

Sea level and its behaviour has been a concern for coastal and other communities for a long time, and hence its measurement has a long history. Sea level association with movement of the moon and sun (IOC, 1985; Pugh, 1987; Emery and Thomson, 2004) thereby producing regular tidal variations was a great innovation, commencing with Newtonian theory. With the advent of modern ocean science technology, the shape of the geoid was established and is now used as a bench mark to measure the sea level variability (Emery and Thomson, 2004).

According to Pugh (1987), the geoid is the shape that the surface of the oceans would take under the influence of Earth's gravity and rotation alone, in the absence of other influences such as winds and tides. All points on that surface have the same scalar potential, i.e., there is no difference in gravitational potential energy between any two adjacent points on an equipotential surface. In other words, the geoid is the equipotential surface that would coincide with the mean ocean surface of the Earth if the oceans and atmosphere were in equilibrium, at rest relative to the rotating Earth, and extended through the continents (such as with very narrow canals). Along the coast the mean sea level (MSL) can be easily measured against a known coastal datum, but far away from the coast it is more difficult to establish.

The sea surface is commonly referred to as mean sea level (MSL), but because the ocean surfaces are not “flat”, this sea surface is not changing globally at the same rate. Mean sea level is the average level of the sea, usually based on hourly values taken over a period of at least a year. The common practice takes into account a need to eliminate the short term changes forced by tides and surges in order to avoid introducing high frequency variations from days to weeks (Pugh, 1987). The same author reports that the MSL can be calculated by

using different approaches such as arithmetic mean values, low-pass filtered mean values, 3-hourly values or mean tide levels.

For geodetic purposes the mean level may be taken over several years which imply that the term mean sea level can also refer to a tidal datum, or frame of vertical reference defined by a specific phase of the tide (Emery and Thomson, 2004).

Tidal datums are locally-derived based on observations at a tide station, and are typically computed over a 19-year period, known as the National Tidal Datum Epoch (NTDE). The present 19-year reference period used by National Oceanic and Atmospheric Administration (NOAA) is the 1983-2001 NTDE. Tidal datum's should be updated at least every 20-25 years due to general global sea level rise/fall. Some stations are more frequently updated due to high relative sea level trends. Tidal datum's are the basis of marine boundaries, which are used as a vertical reference plane in producing nautical charts, and provide important baseline information for observing changes in sea level over time (Pugh, 1987; Emery and Thomson, 2004).

Nevertheless, the Intergovernmental Oceanographic Commission (IOC) manual (1985) and Pugh (1987), argue that at any specific time or location the measured sea level height is composed of three components: the tide (gravitational tide), the weather induced fluctuations (meteorological residuals) and the mean sea level. Each of the three components can be defined in many ways and their variations are independent of each other, as well as the physical processes behind them. The equation 2.1 shows the sum of the three components as described by Pugh (1987):

$$Z_t = Z_0 + X_t + S_t \tag{2.1}$$

Where, $Z_t$ is the observed sea level height, $Z_0$ is the mean sea surface level component, $X_t$ is the gravitational tide component and $S_t$ is the meteorological residuals component.

So, basically the gravitational tides and the weather, according to Pugh (1987), independently govern changes in the sea level and it is known that the regular contribution of tides is much more predictable than the weather effects. The temporal and spatial variations of the sea level are more pronounced hence requiring more refined techniques to detect their proportion of the

changes. It can be achieved just when analysing a time series. The techniques used depend on the objectives of each study that's why they will not be listed here.

Coastal tide gauge records play an important role in studying the temporal and spatial variability of sea level changes. Using tide gauge records, relative sea level trends can be investigated allowing an understanding of changes in local sea level at a range of time scales from decades to centuries. This is important for many coastal applications, including coastal mapping, marine boundary delineation, coastal zone management, coastal engineering, sustainable habitat restoration design, and the general public enjoying their favourite beach (Pugh, 1987). A temporal analysis of the sea level variability can distinguish between both short and long period changes.

### 2.1.1 Sea Level Variability on a short time scales

Sea level variability on short time scales, i.e., less than an hour to months is associated with wind driven surface waves, gravitationally forced tides and seasonal and interannual variations of solar heating. Wind waves have an effect on sea levels on a relatively shorter time scale through their “wave setup” and can affect wide areas. Gravitational tides usually generate sea level variability at semi-diurnal, diurnal, fortnightly, and monthly time scales. Solar heating causes fluctuations in the salinity and temperature distribution in the upper layer of the ocean. Short-term sea level changes also include variability caused by changes in the atmospheric pressure, the winds along the coast, the river runoff and the changes in the large-scale oceanic circulation (Pugh, 1987; Emery and Thomson, 2004). This sea level variability with periods between 3 - 10 days is related to the meteorological forcing and oceanographic response, and is referred to as low frequency variation, according to CTW dynamics which can be determined using daily mean sea level adjusted for the atmospheric pressure (e.g. Brundrit, 1981).

### 2.1.2 Sea Level Variability on a long time scales

Sea level variability on long time scales is due to various factors which affect the volume or mass of the ocean. Among these factors, the changing mass of the ocean and the increase in temperature are two primary causes. The fluctuation of the mass of ocean is influenced by the water locked up on land and as fresh water in rivers, lakes, land glaciers, polar ice caps, and sea ice. The fluctuations in temperature cause changes in the sea water density and as result, can initiate volume expansion or contraction. Very long-term sea level variability has also been due to glacial isostatic rebound and changes in the shape of oceanic basins and in land–sea distribution (Pugh, 1987; Emery and Thomson, 2004; Millar and Douglas, 2004).

### 2.1.2 Previous studies on Sea Level Variability

Few studies have been devoted exclusively to the study of the variability of sea level around southern Africa. The first sea level studies around the coast of southern Africa have been discussed by Brundrit (1984) along the west coast. His studies focused on the seasonal and long-term components of sea-level variability. As conclusion, he said that the seasonal response at the northern and southern ports is clearly different due to the difference in winds affecting these two regions. At all ports, the long-term component was found to be similar suggesting large-scale, non-local forcing. In many cases the sea level variability is part of the investigation of the sea level rise and its impact in both the local and global level provoked by global warming (Pugh, 1987; Hughes, 1992; Brundrit, 1995; Mather, 2007). The aforementioned variability is, actually, in the scope of longer term variability (e.g. Church et al., 2008).

## 2.2 Coastal Trapped Waves: Background

In the ocean, the shelf and coastal zones are very dynamic when compared to offshore. Good vertical measurements are required to determine its stratification. This is the result of higher variations of water temperature, salinity, sea levels, currents and the ocean forcing **(**Tomczak, 1998). The figure 2.1 below shows a typical cross-section of a continental margin.

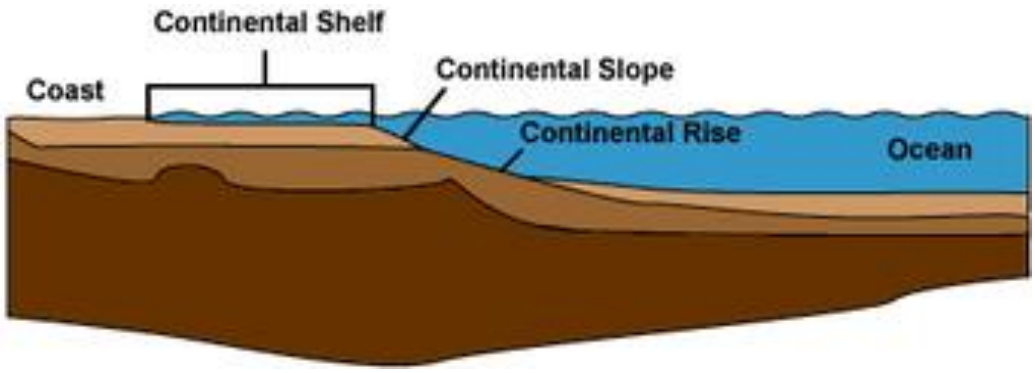


Figure 2.1: Cross-section of the continental margins. The different tones of the brown colour indicate sediment (light brown), rocks (middle brown) and the mantle of the earth (dark brown) – after (http://www.onr.navy.mil/Focus/ocean/regions/oceanfloor2.htm).

CTWs do not fit into the general class of ocean variations mentioned above; rather they belong to the class of height and current variations caused by features of the continental shelf and coastline itself. CTWs are waves which propagate towards the equator on the western boundary of the oceans and towards the poles on the eastern boundary of the oceans, have periods of days to weeks, vertical height variations of the order of 50 cm, and are mainly driven by fluctuations in the longshore component of the wind. CTWs are a mechanism by which winds in one location can influence the coastal ocean at other locations considerably further along the shelf-so called “free waves” **(**Tomczak, 1998).

As is well known, in the open ocean, steady currents are basically dominated by geostrophy, i.e. a zero order balance between oceanic pressure gradient forces and the Coriolis acceleration per unit mass. Regions of high and low sea levels create the geostrophic balance, and these are generally referred to as “high and low pressure” centres. In the southern hemisphere, the high pressure centres always have an anti-cyclonic (anti-clockwise) flow, while the low pressure creates a cyclonic flow. When the high and low pressure centres are in close proximity to the coastal ocean, they can cause the water to move from one side of the shelf to the other, an effect that can easily be seen as the lowering and rising sea level at the coast. The aforementioned effect, lowering and rising of the sea level also means changes in pressure. The effect of these changes can then be seen as ocean currents flowing parallel to the coast **(**Tomczak, 1998).

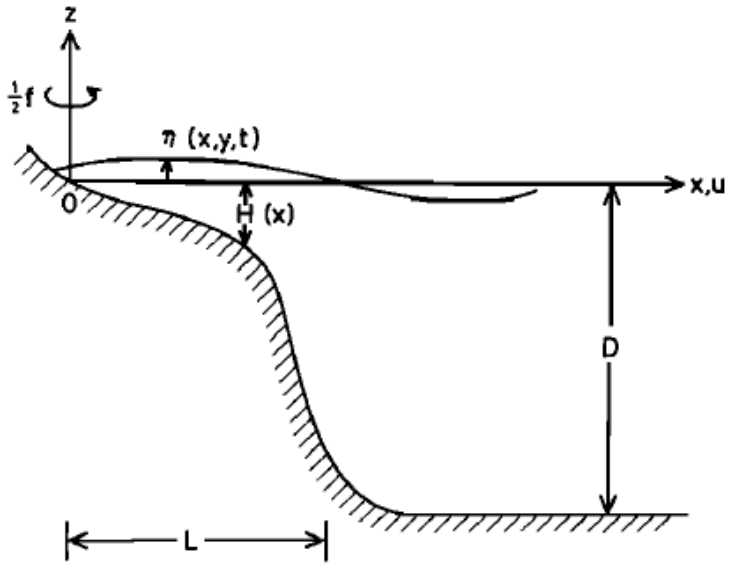


Figure 2.2: Schematic diagram of the shelf with the variables usually used to define the CTWs in the northern hemisphere – after Mysak (1980). The y axis and y velocity component v are directed into the plane at 0 and are along the mean coastline. L is the sloping continental shelf width, H(x) is the depth variation and D is the mean deep-sea depth far from the coast.

Therefore, the moving water in the presence of a shelf is truly a propagation of a wave known as coastal trapped wave (CTW). The existence and propagation speed of CTWs depends largely on the nature of the continual shelf depth, width, and slope. A combination of these details can act in order to favour or inhibit the CTW's life after it has left the area of formation **(**Tomczak, 1998). Figure 2.2 shows the coordinate system used to discuss the propagation characteristics of the CTWs along the continental shelf-slope area. The CTWs will have different motion characteristics depending on if the shelf is wide (L > 100 Km) or narrow (Emery and Thomson, 2004). Usually, the propagation of the CTWs will be fast or slow when the shelf is narrow or wide, respectively, though it sometimes depends also on the speed of propagation of the forcing mechanism. Emery and Thomson (2004), also argue that the CTWs motions will be based on the continental slope when the shelf is wide and at the coast when the shelf is narrow, tending to elongate the flow against the coastal boundary.

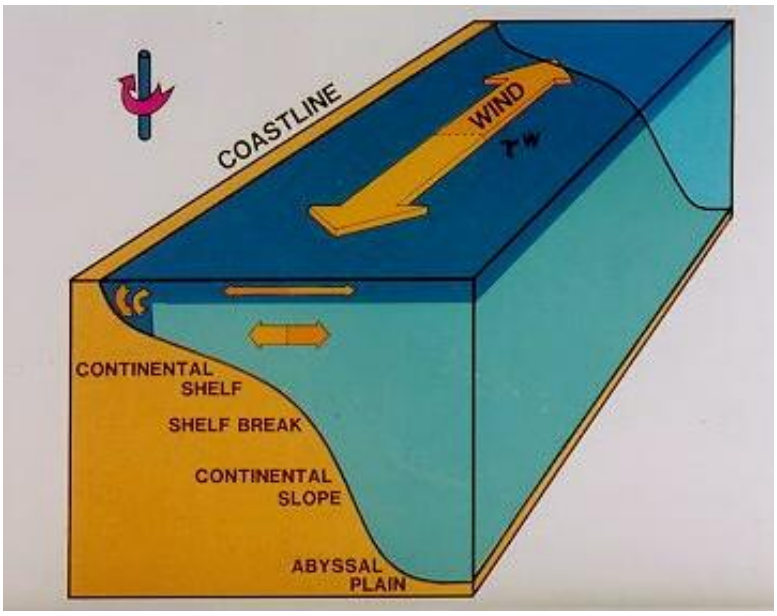


Figure 2.3**:** Schematic diagram of the basic conditions for the emergence of coastal trapped waves – after Tomczak (1998). The needs for that are the earth's rotation, displayed in the upper left of the diagram, a continental shelf-slope and the action of an external forcing such as a periodic alongshore component of the wind stress depicted by $\tau^w$.

The origin and the presence of CTWs is well explained when wind is taken as the forcing mechanism. Assume that the wind is blowing, in the same position along the coast with a periodic variation in longshore direction i.e., in the same direction but opposite sense, in time. This will produce a periodically changing forcing on the coastal ocean. In the shallow region of the ocean, the combined effect of earth rotation and wind stress will produce upwelling and downwelling near to the coast as result of an Ekman layer. The Ekman layer is also known as the surface mixed layer, and will vary in magnitude according to the nature of the sloping bottom of the shelf. Because of the Earth's rotation, the shelf waters it carry angular momentum which is conserved **(**Tomczak, 1998), see Figure 2.3.

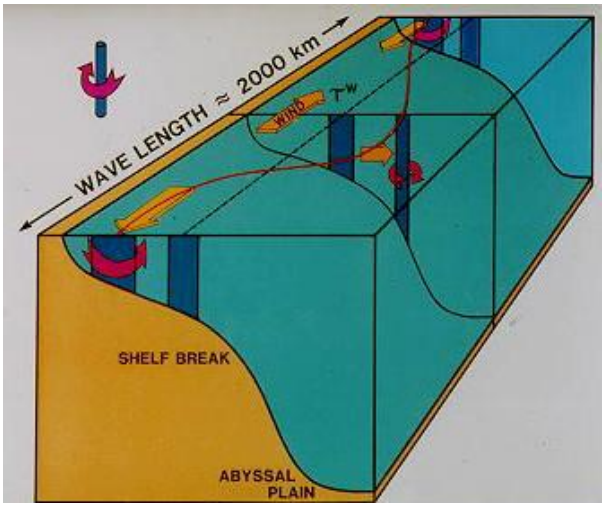


Figure 2. 4: The effect of downwelling or upwelling on the coastal ocean in the southern hemisphere – Tomczak (1998). Due to the wind stress on the surface mixed layer, downwelling and upwelling pushes and pulls the water below the mixed layer away from and towards the coast, respectively. The result is a negative and positive vorticity, in this case, at a location depicted by the red line. Note that the mixed layer was removed on the diagram to illustrate what happen below it.

Below the Ekman layer, vorticity conservation results in both offshore and onshore movement of a water column. In response to the downwelling and upwelling, negative and positive vorticity alternate in order to remove and replace water (see Figure 2.4) which in the end will cause equatorward or poleward movements of the water particles according which coast is being considered **(**Tomczak, 1998). Figure 2.4 illustrates the resulting adjustment in the water column, where a northward propagating wave can be seen along an east coast in the southern hemisphere.

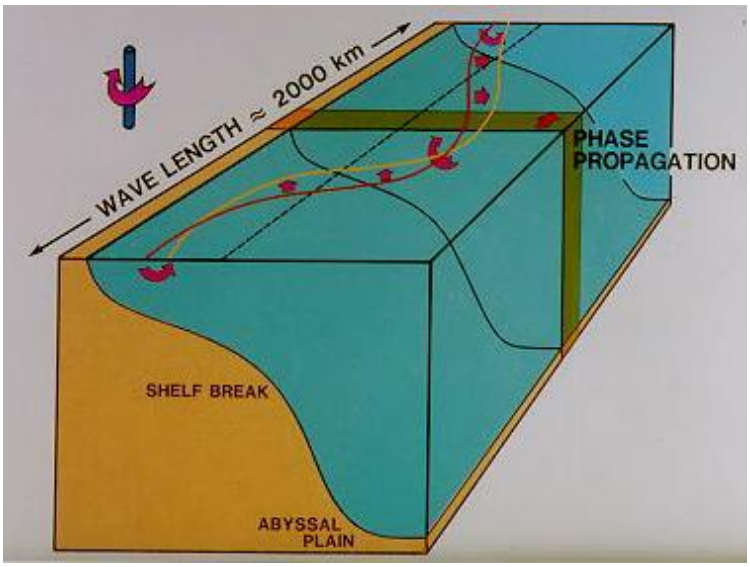


Figure 2.5**:** The general picture after a periodic alongshore wind event due to the conservation of the vorticity in the southern hemisphere – after Tomczak (1998). The red line is the position of the water particles before the forcing whereas the yellow line represents the new position, after forcing event.

According to Tomczak (1998), the water particles movement appears like wave propagation which is coastal trapped wave propagation, Figure 2.5. Observation shows that CTWs behaviour is similar to Kelvin waves; the main difference is that the shelf slope is crucial for CTWs and a vertical shelf or equator are required for Kelvin waves. (Tomczak, 1998; Emery and Thomson, 2007). The cross-shore characteristics are defined by the density structure and length scale of the topography (Emery and Thomson, 2007). Because they are shelf dependent, their wave profile changes according to the season which makes them one of the most important objects of study in the observed sea level variability and currents **(**Tomczak, 1998).

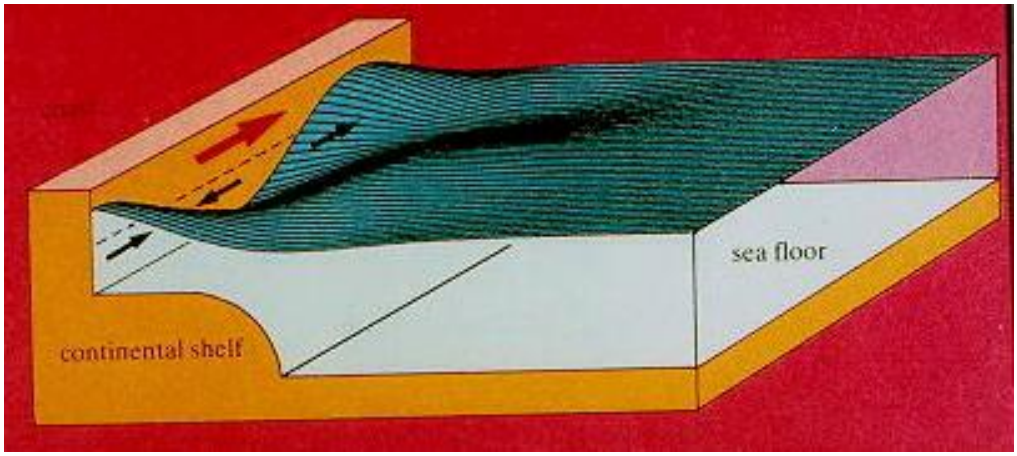


Figure 2.6: The resulting deformation which actually is a wave – after Tomczak (1998). The figure shows the dependence of the wave on the cross shelf structure. It has the largest amplitude at the coast, and decays exponentially towards the shelf break. There is no height variation in the deep ocean.

## 2.2.1 Coastal Trapped Waves: Brief history

Sir William Thompson (who later became Lord Kelvin) is the person who developed the ideas behind "Kelvin waves" in 1879. Thomson (1879) showed that in the ocean or atmosphere there are waves which depend on the Coriolis force, the gravitational attraction and the simple "flat bottom" ocean with a vertical wall. This wave, which afterwards was given his name, moves toward the pole along an eastern boundary, equatorward along a western boundary, and counter-clockwise in the open ocean in the Northern Hemisphere or clockwise in the Southern Hemisphere. Boundary trapped and equatorially trapped Kelvin waves are two groups that can be found. Each group can then be subdivided into surface (barotropic) and internal (baroclinic) Kelvin waves. Internal Kelvin waves as well as coastal Kelvin waves (CKW), present some of the key dynamics for the study and understanding of the fundamental theory behind coastal trapped waves on a gently sloping continental shelf.

Early analysis of low frequency sea level residuals remaining after the tides had been removed showed that at some stations there was a deviation from the simple inverse barometer theory. Robinson (1964), tried to find an answer for this, and developed the first numerical analysis of CTWs. His study was centred on the response of the continental shelf sea level to weather systems along Australian coast using shallow water equations for a rotating fluid developed by Thomson (1879). The CTW is a dispersive wave solution with a shelf topography

connecting to a homogenous ocean at rest. The solution is governed by potential vorticity conservation and propagates along the coast always having the coast on its left side in the southern hemisphere. Hamon (1966) associated the observed signals at tide gauges along the coast with a continental shelf wave (CSW) or CTW with an estimated phase speed of about 4 m/s. These CTW signals were a result of comparing the time lags in the adjusted sea level between neighbouring coastal stations.

Mysak (1967), in his work on the theory of continental shelf waves, investigated waves along coasts in a two layer ocean at coast of Australia. Based on the previous studies and analysis conducted by Robinson (1964), he tested new assumptions in order to reconcile the mathematical results with the theory of CSW. For him there were some discrepancies in Robinson's model. His disagreement with Robinson was centred on the fact that the Robinson solution does not take into account the link between the sea level variation patterns and the latitude as well as the weather system motion contribution. As result, he found a wave solution that propagates along a coast in a direction with the coast located on the left side in the southern hemisphere or on the right side in the northern hemisphere. He suggested also that during its propagation, the CSW can be influenced by the shelf slope, the deep sea stratification and the background current flow direction.

Gill and Clarke (1974) in their study of wind-induced coastal currents and sea level changes, suggested the tide gauge as a reliable source of information about upwelling and coastal currents. Discussing the effects of shelf topography and density stratification on the coastal upwelling and taking into consideration the assumption brought by Mysak (1967), they proposed the name costal trapped waves (CTWs) for the first time instead of coastal Kelvin waves (Thomson, 1879) or continental shelf waves (Robinson, 1964); names which at that time were commonly used. Coastal trapped waves became the appropriate appellation since they possess hybrid characteristics between the CKW and the CSW.

Thus a new field of study in physical oceanography was starting. The study carried out by Gill and Clarke (1974) led to numerous investigations of the existence of costal trapped waves (CTWs) along various coastlines around the world. Some of the investigations are reviewed here.

#### 2.2.1.1 Investigations of coastal trapped waves along various coastlines around the world

The first investigations of the existence of CTWs were primarily based on the hourly measurements of sea level recorded by tide gauges. With time, detailed current measurements were also analysed to improve the mathematical models. Most recently, satellite altimetry measurements are also being used. The monograph by LeBlond and Mysak (1978), Mysak (1980) or Reynaud et al. (1991) gives an excellent review of studies conducted up to that time.

Maiwa et al. (2009) investigated the spatial variations and propagation characteristics of CTWs along the western, southern and eastern coasts of Australia. They used 20 tide gauge records, for the observations, and the output from a high-resolution ocean general circulation model (OGCM) to simulate the CTWs. With the observed sea level data, the CTWs were found propagating anticlockwise around the Australian coast. The signal shown by the data is faster on the western and southern coasts and slower along the eastern coast. It is basically forced by the longshore wind in the south-western and south-eastern regions. This result was confirmed by the numerical model simulations. The OGCM reproduced the CTWs signal remarkably well. The analysis in this thesis uses a similar methodology to that of Maiwa et al. (2009).

#### 2.2.1.2 Investigations of coastal trapped waves around southern Africa coast

There are only a few studies along the southern Africa coastline, most of which are confined to the South African coast. Gill and Schumann (1979) found small currents which act in the opposite way to the Agulhas Current. They developed the hypotheses as to why the CTWs were likely to be absent along the very narrow east continental shelf. The hypotheses consisted of considering the situations that involve the flow of an inertial jet along a coastal boundary, where the basic premise was the conservation of potential vorticity in various layers as the current moves into different regimes. The nature of the jet has been altered by changes in both the local vertical component of the Coriolis parameter $f$ and topographic changes. Moreover, the approach assumed and used concentrates on the structure of the inertial current, where its path is well defined because it is constrained to follow a boundary.

de Cuevas et al. (1986) carried out an empirical study of the low-frequency sea level fluctuations using one year (1982) of tide gauge records from nine ports along the coasts of Namibia and South Africa. They found that the CTWs were associated with synoptic weather systems. Based on the examination at adjacent ports, they found that the CTW signal moves anticlockwise southwards from Namibia on the west coast to south coast and mostly disappearing somewhere between Port Elizabeth and Durban on the east coast.

Schumann and Brink (1990) revisited the measurements of CTWs around southern Africa, and conducted a study with the purpose of determining the generation, propagation and current structures of CTWs along the coast of South Africa. Their data consisted of observed sea levels measurements from 6 coastal sites as well as a few current measurements over the shelf. They concluded that anticlockwise perturbations found can be identified as CTWs but recognised some disagreement between data results and literature due to Agulhas Current along the east coast. Their results suggest that the CTWs are inhibited by the Agulhas Current, as was previously reported by de Cuevas et al. (1986), on their eastward and equatorward propagation. The main wind forcing and variation of the shelf topography along the wide west and south coast continental shelves had a profound effect on the CTWs.

## 2.2.2 Formulation of the coastal trapped waves

The following description of the coastal trapped waves takes into account the shelf topography and stratification, e. g. Mysak (1980), Brink (1990), Maiwa et al. (2009). Consider a stratified ocean which overlies shelf topography. Choose the *y* axis along the coast, *x* axis perpendicular to the coast and *z* axis vertically upward from the ocean surface. Consider a linear, inviscid problem with constant rotation under the Boussinesq and hydrostatic approximations. Then, assuming the time scales are much greater than an inertial frequency and the *y* scale of the motion is much greater than the width of the shelf and slope, the equations of motion are:

$$-fv = -\frac{1}{\rho_0}\frac{\partial p}{\partial x} \tag{2.2}$$

$$\frac{\partial v}{\partial t} + fu = -\frac{1}{\rho_0}\frac{\partial p}{\partial y} \tag{2.3}$$

$$\rho\, g = -\frac{\partial p}{\partial z} \tag{2.4}$$

$$\frac{\partial u}{\partial x} + \frac{\partial v}{\partial y} + \frac{\partial w}{\partial z} = 0 \tag{2.5}$$

$$\frac{\partial p}{\partial t} + w\frac{\partial \overline{\rho}}{\partial z} = 0 \tag{2.6}$$

Where $u$, $v$ and $w$ are the offshore, alongshore and vertical velocity components, $\rho'(x, y, z, t)$ is the density perturbation from a rest state $\rho$ $(z)$, $p$ is the pressure perturbation, $f$ the Coriolis parameter, $g$ the acceleration due to gravity, and subscripts $(x, y, z, t)$ denote partial differentiation. The system (2.2), (2.3), (2.4), (2.5) and (2.6) reduces to:

$$\frac{\partial^3 p}{\partial x^2 \partial t} + f^2 \frac{\partial}{\partial}\left(\frac{1}{N^2}\frac{\partial^2 p}{\partial z \partial t}\right) = 0 \tag{2.7}$$

where the Brunt-Väisälä frequency is defined as:

$$N^2 = -\frac{g}{\rho_0}\frac{\partial \overline{\rho}}{\partial z} \tag{2.8}$$

The appropriate boundary conditions are:

$$g\frac{\partial p}{\partial z} + N^2 p = 0 \quad \text{at} \quad z = 0 \tag{2.9}$$

$$f\frac{\partial p}{\partial z} + \frac{\partial^2 p}{\partial x \partial t} = 0 \quad \text{at} \quad x = 0 \tag{2.10}$$

$$f^2\frac{\partial^2 p}{\partial z \partial t} + N^2\left(f\frac{\partial p}{\partial y} + \frac{\partial^2 p}{\partial x \partial t}\right)\frac{\partial h}{\partial x} = 0 \quad \text{at} \quad z = -h \tag{2.11}$$

$$p = 0 \ \text{ at } \ x \to \tag{2.12}$$

where $h(x)$ is the local depth of the ocean. The first condition represents a free surface, while the second and third follow from no normal flow at a coastal wall and at the bottom, respectively. The final condition expresses coastal trapping.

In order to find the free coastal trapped waves, assume the travelling wave and vertical, across-shore modal solution $F_n(x, z)$ of (2.7) as:

$$p = \sum_{n=1} F_n(x,z) exp\big(i(l_n y + wt)\big) \qquad (n = 1,2, \dots) \tag{2.13}$$

Substituting (2.13) into (2.7) to (2.12), this system becomes a two-dimensional eigenvalue problem:

$$\frac{\partial^2 F_n}{\partial x^2} + f^2 \frac{\partial}{\partial z}\left(\frac{1}{N^2}\frac{\partial F_n}{\partial z}\right) = 0 \qquad (n = 1,2, \dots) \tag{2.14}$$

$$g\frac{\partial F_n}{\partial z} + N^2 F_n = 0 \quad \text{at} \quad z = 0 \tag{2.15}$$

$$f c_n^{-1} F_n + \frac{\partial F_n}{\partial x} = 0 \quad \text{at} \quad x = 0 \tag{2.16}$$

$$\frac{\partial F_n}{\partial z} + \frac{N^2}{f^2}\left(\frac{\partial F_n}{\partial x} + f c_n^{-1} F_n\right)\frac{\partial h}{\partial x} = 0 \quad \text{at} \quad z = -h \tag{2.17}$$

$$F_n = 0 \quad \text{at} \quad x \to \tag{2.18}$$

where ($c_n = \omega/l_n$) is a phase speed of the $n$-th mode.

## 2.3 Meteorology around southern Africa coast

The large scale weather systems that dominate the winds on the southern Africa coasts are the same which generally affect the southern African continent e.g. Taljaard (1972); van Loon (1972). While Preston-Whyte and Tyson (1988), and Tyson and Preston-Whyte (2000) focused their studies just on the southern Africa. Specific study regarding to the coast are fewer.

Duncan (1970) in his research on the Agulhas Current described in detail the east coast meteorology. Nelson and Hutchings (1983) characterized the typical South African west coast meteorology, describing the nature of passing extra tropical cyclones, coastal lows and the semi-permanent high pressure systems. The essential detail from these studies is highlighted.

The wind fields around the southern Africa coast are regulated in the west by the St Helena anticyclone situated over the South Atlantic Ocean, and in the southwest Indian Ocean by the Mascarene anticyclone. Both systems have a southward displacement in summers, and so present a seasonal variation through the year. The Inter-tropical Convergence Zone (ITCZ) also displays a seasonal and an interannual north-south migration.

In summer, the core of the anticyclone centres are situated more southward around $34^{o}$ S. As a result, the westerlies are situated in the south far away the continent and, they may influence the western, southern and south-eastern coastal areas only when the winds are strong. In the west, the winds are often strong and persistent over a few days to weeks. They are frequently south or south-easterly in summer, due to the ridging of South Atlantic high pressure gradients south of Africa. The south-eastern part of the region is mostly dominated by the north-eastern trade winds of the South Indian high pressure system (in summer). In the far north-eastern part of the region, tropical cyclones occasionally move westwards through the Mozambique Channel, but mainly curve southwards over the southwest Indian Ocean east of the Madagascar. The sustained winds in these storms frequently exceed hurricane force.

In austral winter, the centres of the high pressure systems move latitudinally about six degrees equatorward from their location in summer. As result, the main features, as described for the summer, remain the same mostly in the north of the centres of the high pressure systems. Westerlies associated with the eastward moving mid-latitude depressions from the south-west Atlantic, reign in the south of the core of the anticyclone centres, near Port Nolloth. Cold fronts often move over these areas and may reach far to the north. When the South Atlantic high pressure system moves more eastwards and stays strong, gale force winds can spread to the south-east coast as far north as the Mozambique Channel.

# CHAPTER 3

# DATA AND METHODS

## 3.1 Study area

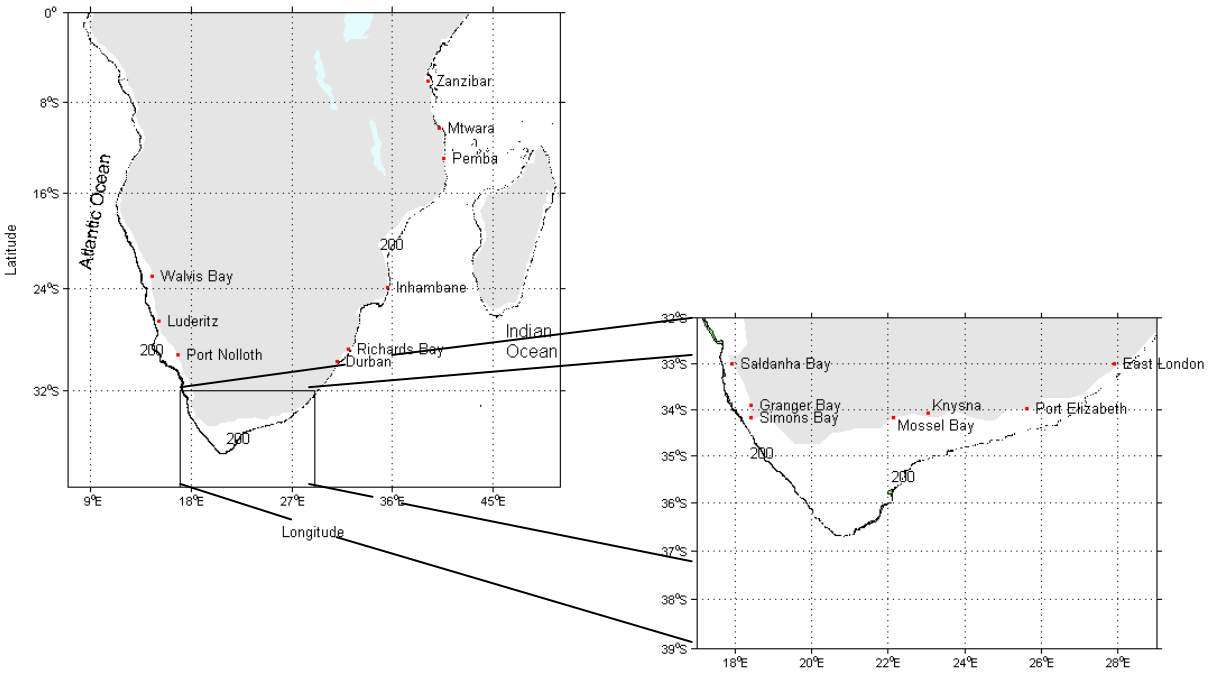


Figure 3.1: Location of tide gauges considered for this study (stations are labelled with their names) and bathymetry (m) of southern Africa; the 200 m isobath marks the approximate position of the shelf break.

## 3.2 Data

In this study, three types of data were used, namely: observed, satellite and model data. The observed records are the main data in this study. Satellite derived observations were used due to the absence of *in situ* measurements of some parameters involved in this study. Model data were used in order to, when it shows good results, utilise them in future for studying sea level variability with more confidence. Below is the detailed information concerning each parameter used in this study.

### 3.2.1 Tide gauge records

Tide gauge records are observed daily mean sea level, provided by the University of Hawaii Sea Level Centre (UHSLC), in millimetres (mm) at 16 tide gauges around Southern Africa (figure 3.1), for the period from 1 January, 2008 to 31 December, 2010 (table 1). The data sets are research quality data, more information can be found at: http://www.uhslc.soest.hawaii.edu.

### 3.2.2 Air pressure records

Daily surface air pressure records in Pascal's (Pa) with 2.5 degree resolution in both latitude and longitude were taken from the National Centre for Environmental Prediction (NCEP)/ National Centre for Atmospheric Research (NCAR) provided by the National Oceanic and Atmospheric Administration (NOAA) - Cooperative Institute for Research in Environmental Sciences (CIRES) Climatic Diagnostics Centre, for the period from 1 January, 2008 to 31 December, 2010. More details and description about the data sets are available from the link: http://www.esrl.noaa.gov/psd/data/gridded/data.ncep.reanalysis.html .

### 3.2.3 Winds

The wind data sets are from two providers. As result two different spatial resolutions were used at two different stages of the study.

#### Seawinds

To compute the alongshore wind, daily wind velocity datasets, in metre per second (m/s), at 10 m above the sea were taken from "NOAA NESDIS National Climatic Data Centre" for the period from 1 January, 2008 to 31 December, 2010. The data are provided with 0.25 degree resolution in both latitude and longitude. More information can be found at http://www.ncdc.noaa.gov/oa/rsad/blendedseawinds.html.

NCEP/NCAR Reanalysis winds

To visualize and understand the wind forcing, NCEP/NCAR Reanalysis winds were superposed on the sea level pressure. The datasets are daily with 2.5 degree resolution in both latitude and longitude, at 10 m above the sea/land surface from the NCEP/NCAR provided by the NOAA - CIRES Climatic Diagnostics Centre, for the period from 1 January, 2008 to 31 December, 2010. More details and description about the data sets are at the link: http://www.esrl.noaa.gov/psd/data/gridded/data.ncep.reanalysis.html .

### 3.2.4 Sea Surface Heights from the Hybrid Coordinate Ocean Model (HYCOM) for southern Africa

Daily mean sea surface heights from the Hybrid Coordinate Ocean Model (HYCOM), version 2.2 (Wallcraft et al., 2009), for southern Africa were used to compare with the results from the observed data. HYCOM is a primitive equation general circulation model which is able to interchange between different vertical coordinate schemes. It is isopycnal in the open, stratified ocean, but smoothly reverts to a terrain-following coordinate in shallow coastal regions, and to z-level coordinates in the mixed layer and/or unstratified seas. HYCOM is designed to provide a major advance over the existing operational global ocean prediction systems, since it overcomes design limitations of the present systems as well as limitations in vertical and horizontal resolution (Bleck, 2002; Wallcraft et al., 2009; George et al., 2010; Backeberg et al., in press).

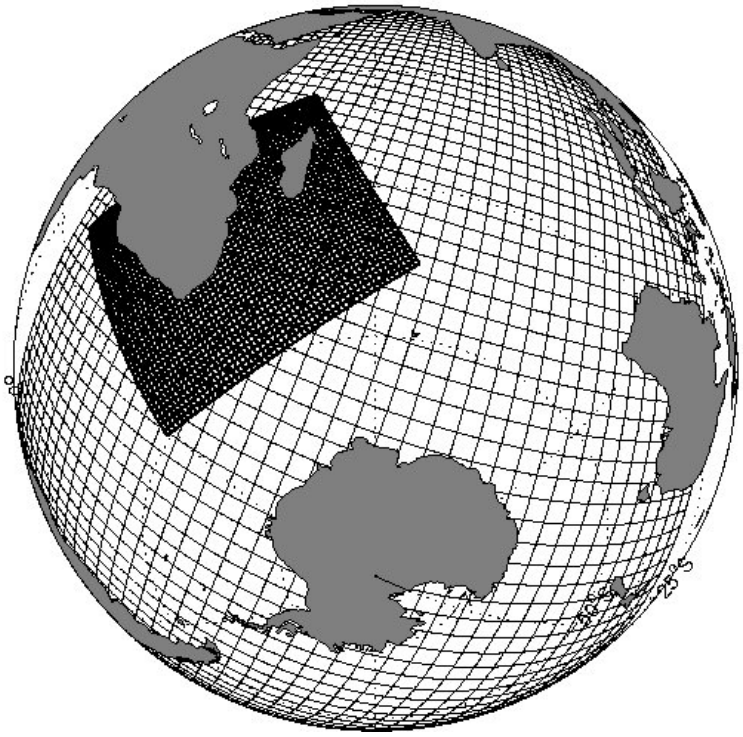

Figure 3.2: The configuration of the domains in the HYCOM model system after Backeberg, 2009. Coarse resolution basin-scale of the outer model grid, provides boundary conditions for a high-resolution inner regional model grid. Every tenth grid point was plotted to produce the respective mesh grids, therefore each box consists of 10x10 grid cells.

The model employs two domains (figure 3.2), the outer model with the horizontal resolution gradually decreasing from 14 km in the northern Indian Ocean, around India, to 42 km in the southern part, around Antarctica (e. g. Backeberg, 2009; George et al., 2010; Backeberg et al., in press), while the resolution of the inner model is $1=10^0$ (10 km) (e. g. Backeberg, 2009; Backeberg et al., in press). The resolution of the inner model, according to Backeberg, 2009, is sufficient enough to include important features of the Agulhas Current system such as the Mozambique Channel and the East Madagascar Current, the Agulhas Current core, the Agulhas retroflection, the ring shedding corridor and the Agulhas return current (figure 3.3).

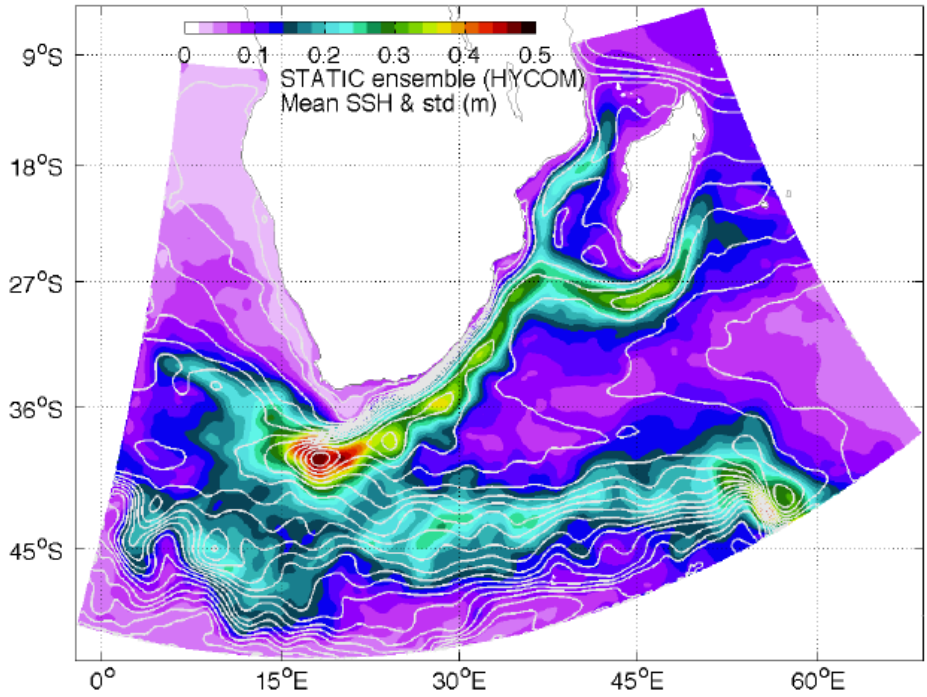


Figure 3.3: The regional HYCOM of the Agulhas region domain and the configuration of its outputs after Backeberg et al. (in press). Mean sea surface height (white contours ranging from – 1 m to 1.5 at 10 cm intervals) and its standard deviation (colour scheme) of the regional HYCOM of the Agulhas. The mean and standard deviation are calculated for the period 1998 – 2007 corresponding to the period from which the static ensemble is generated.

Both the inner model and outer model were created using a conformal mapping tool (Bentsen et al., 1999). The inner model receives boundary conditions from the outer model based on the Newtonian relaxation in sponge layers and full open-ocean boundary conditions (Wallcraft et al., 2009; George et al., 2010). The horizontal resolution of the inner model is sufficient for eddy resolving since the Rossby radius of deformation (Chelton et al., 1998) is about 30 km.

Both models use 30 hybrid layers spaced with a minimum of 3 m in the top layers using reference density $\sigma_0 = 1000\, kg.m^{-3}$ for target densities ranging from 21.0 to 28.3 (Backeberg, 2008; Backeberg, 2009; George et al., 2010; Backeberg et al., in press).

Levitus climatology (Locarnini et al., 2006; Antonov, 2006) is used to initialize the outer model and, 10 years spin up period was run to reach equilibrium using ERA-interim forcing (Dee et al., 2011). After this equilibrium, the inner model is then initialized, interpolated to the high resolution grid (Backeberg, 2008; Backeberg, 2009; Backeberg et al., in press).

The atmospheric forcing fields for a period 1980 – 2007 from ERA-interim reanalysis data provided by the European Centre for Medium-Range Weather Forecasts (ECMWF) are used to run both models (Backeberg, 2008; Backeberg, 2009; Backeberg et al., in press). The momentum and the heat fluxes are calculated from bulk formulas. Rivers runoff are considered as a negative salinity flux where they are determined using the hydrological model called TOTAL Runoff Integrating Pathways (Oki and Sud, 1998).

## 3.3 Methodology

MATLAB 2011b and Microsoft Excel 2007 were used to analysis the data. MATLAB is a numerical computing environment and fourth generation programming language; see http://www.mathworks.com/products/matlab/ links within for details and description of Microsoft Excel can be found at http://www.office.microsoft.com/en-us/excel.

### 3.3.1 Time range of the tide gauge records

The sequential data at each tide gauge station presents several data gaps or "jumps". So for the observed sea levels there was a need to find the best time period for the analysis. To do so, priority was given to the stations located in the west and south regions of southern Africa. The reason for that is because is believed that the west plays an important starting point occurrence of CTWs around southern Africa (Shillington, pers. Comm.). In addition, the best evidence of the occurrence of CTWs can be found along the south coast. Priority also took into account that the previous studies were done for both of these two regions which will allow the comparison of the final results from this study. To define the best time range the east coast region was the last to be included.

Although the de Cuevas et al. (1986) had already included the east region until Richard's Bay, in this study the area was extended to Zanzibar, in Tanzania, in order to get more detailed information. The eastern region is the one which will hopefully produce a novel difference between this study and the previous publication. Therefore, with the east region will be the

key to try to answer questions or doubts left by the previous studies, particularly from Port Elizabeth to Inhambane.

Thus, taking in to consideration the numbered reasons aforementioned a period of three years presented good sequential data (table 1) which allowed working with 16 tide gauges. Figure 3.1 shows the locations of those tide gauges and the bathymetry around southern Africa.

To visualize the data for the observed sea levels around the coast of Southern Africa, and hence examine the patterns of their variability, plots were made for each of the 16 single tide stations, which at same time revealed the data gaps present. Visual examination helped to identify these gaps as part of quality control. Another technique used is the spectral analysis of the daily tide gauge data (Emery and Thomson, 2004) in order to show the power/frequency domain of the time series. This was done section by section of continuous data. In this way, the results come out without any gap contamination. So the section with longer continuous datasets was taken as representative of each tide gauge station.

Missing data values up to a maximum of 10 consecutive days were then filled by linear interpolation (Hodnesdal, 2006; Maiwa et al., 2009) for each tide gauge time series. Most interpolation methods rely on the data characteristics, the number of points being replaced and some suitable mathematical criteria (Emery and Thomson, 2004). Linear interpolation is the simplest way to calculate new value using the given set of values. According to Emery and Thomson (2004) linear interpolation is deeply employed worldwide, it uses linear polynomials while fitting the curve with the desired values. The formulation below derived from the Lagrange polynomial interpolation formula (Emery and Thomson, 2004) best fit the situation:

$$y(x) = y(a) + \frac{x-a}{b-a}[y(b) - y(a)] = \frac{(b-x)y(a)+(x-a)y(b)}{b-a} \quad (3.1)$$

Where $x_{start} = a$ and $x_{end} = b$ are times or positions of the data collection at the start and end of the sampling increment being interpolated, and $x$ represents the corresponding time or position of the desired interpolated value within the interval [a, b].

Table 1: Summaries of the source of tide gauge records. Position means the distance approximated relative to Walvis Bay calculated along a smoothed coastline. Data indicate the length of the used datasets at each tide gauge. Range is the difference between maximum and minimum values of sea level height.

| **Location** | | | **Sea level** | | |
|---|---|---|---|---|---|
| **Country** | Tide gauge | | Position | Data | Range |
| | Name | Abbreviation | (km) | (days) | (cm) |
| **Namibia** | Walvis Bay | WB | 0 | 963 | 40 |
| | Luderitz | L | 417 | 843 | 44 |
| **South Africa** | Port Nolloth | PL | 754 | 1096 | 68 |
| | Saldanha Bay | SaB | 1184 | 673 | 59 |
| | Granger Bay | GB | 1294 | 693 | 66 |
| | Simon's Bay | SB | 1325 | 1083 | 55 |
| | Mossel Bay | MB | 1667 | 1022 | 84 |
| | Knysna | K | 1751 | 1066 | 106 |
| | Port Elizabeth | PE | 1990 | 1096 | 82 |
| | East London | EL | 2226 | 1041 | 67 |
| | Durban | D | 2687 | 922 | 58 |
| | Richard's Bay | RB | 2842 | 976 | 59 |
| **Mozambique** | Inhambane | I | 3482 | 99 | 28 |
| | Pemba | P | 4813 | 764 | 51 |
| **Tanzania** | Mtwara | M | 5114 | 360 | 30 |
| | Zanzibar | Z | 5587 | 791 | 27 |

The sea level is amongst one of most useful measurements which integrates the influences of various oceanic processes, that include the effects due to coastal currents, effects due to the field of mass, density, meteorological effects due to radiation, pressure, wind force and direction, evaporation, precipitation, effects due to the Earth's geopotential, the geoid, effects relative to the oceanic boundaries, effects due to the rotation of the Earth, as well as the effects of the tidal forcing due to the astronomical nature of the tides (Pugh, 1987).

### 3.3.1.1 Analysis of short-term sea level variability

There is no aliasing of the CTW signal, as a preliminary plot at higher frequency sampling (hourly) showed similar patterns in time. Thus, daily averages of the hourly data were constructed and plotted on the same axis. Then, visual examination helped decide whether the pattern it showed corresponds to the CTWs according to the theory. It was noted that the

previous studies were carried out using data with the same time frequency i.e., observed daily mean sea level.

Short-term sea level variability over periods of the order of 3 – 10 days is mainly related to the local and remote meteorological and oceanographic forcing (so called low frequency fluctuations). For this study, daily mean sea level adjusted for the atmospheric pressure effect is the chosen data. The main objective of this analysis is to investigate how it's correlated with the local or neighbouring wind and to determine any other low frequency fluctuations not incorporated in the wind (Brundrit, 1981).

Indeed, the sea level variability must take into account the mean sea level. The sea level variability is, for that reason, the deviation in respect to the mean sea level, in other words is the sea level anomaly. The definition assumed comes upon the theory that the variability forced by wind stress and mean air pressures or linked to the CTW, normally, according to Pugh (1987) are unlikely to have amplitudes greater than 50 cm, although Krause and Radok (1976) and, Schumann and Brink (1990) reported amplitudes > 50 cm off the south coast of Australia and southern Africa, respectively.

As was said before, the mean sea level, the tide and the weather are the three components that can be found in any measurement of sea level. There is a need to separate the weather from other two components. To achieve this goal the variability at each tide gauge station was determined by removing seasonal cycles from the observed records. The assumption is that the oceans experience greater summer air pressures and lower winter air pressures and these must be taken into consideration. The results are now assumed as the records that are corrected for the IBE (Pugh, 1987). The records were converted to centimetre (cm) to be adjusted for IBE using surface air pressure datasets. The original values of the surface air pressure are in pascals (Pa), but were converted to millibar (mb).

According to Robinson (1964), the level of the deep oceans should respond to the IBE. This is also known as "isostatic" response to each weather system. We assume from the IBE that 1 hPa increase (decrease) in the atmospheric pressure corresponds to 1 cm decrease (increase) in the sea level (Hamon, 1966; Buchwald and Adams, 1968; Mysak, 1967; Pugh, 1987; Schumann and Brink, 1990; Maiwa et al., 2009; Antunes and Taborda, 2009; Antunes, 2011).

The records were adjusted by formulas described by Pugh (1987), Schumann and Brink (1990) and Antunes (2011):

$$Z_{(t)} = Z_{(t)} - (\overline{AP} - AP) \tag{3.2}$$

Where, $Z_{(t)}$ is the pressure adjusted sea level height in cm, $Z_{(t)}$ is the measured sea level height in cm, $\overline{AP}$ is the mean surface pressure in mb and $AP$ is the actual surface pressure in mb.

So, from now any reference to the observed sea level will imply the adjusted sea level. To visualize the frequency bands of significant energy peaks within the time series, a power spectral analysis approach was used (Brundrit, 1981; Emery and Thomson, 2004).

The power spectrum analysis used is the multi-taper method with adaptive weighting (e. g. Percival and Walden, 1993). There was a need to understand the frequency bands with significant energy peaks within the time series. In order to achieve this, a wavelet analysis was applied. The wavelet analysis is a good technique to find both the frequency bands of significant energy peaks and how these frequency bands of significant energy peaks change in time (Torrence and Compo, 1998). The wavelet power spectrum function used is based on the Morlet wavelet function as described by Torrence and Compo (1998). For both the power spectrum and wavelet spectrum, 95 per cent significance was used as the criterion of significance. Because the data at Inhambane and Mtwara has a lot of gaps, both these stations were excluded from the power and wavelet spectrum analyses.

The propagation characteristics of the CTWs were investigated using Hovmöller diagrams of distance, time and CTW amplitude. This enables one to visualize the propagating signals and to estimate the speed of their propagation along the coast. The typical period is found by calculating the time difference between the peaks within the propagating events at two adjacent station locations. The velocity of propagation can be determined by the slope created when fitting the lines to the propagating signals. A similar approach uses the lag correlation analysis between two points, in this case, two tide gauges (Maiwa et al., 2009).

Plots of the wind stress superposed by the sea level pressure were also produced. This was done because the wind forcing is always linked to the atmospheric pressure perturbations and it is seldom possible to understand the impact of the wind forcing separately (Pugh, 1987). Obviously this exercise is important when examining what was going on during propagating signals.

### 3.3.2 Alongshore winds

Usually along the ocean boundary, the component of a wind stress that acts parallel to the coastline is called the alongshore wind. It produces sea level variability by disturbing the water movements associated with the Ekman transport dynamics (Pugh, 1987). In this study, the alongshore wind at the coast was defined by taking into account the orientation of the coast of each tide gauge station. Thus, to avoid being too rigid on the definition of the alongshore wind at each tide gauge, as well as taking into consideration that the wind varies greatly its direction over time, the alongshore wind used is allowed to have a small range (0.1 degree around the geographical position of the tide gauge) in the wind direction. Using the above data and methods, the results are discussed in the next section.

# Chapter 4

# RESULTS

## 4.1 Characteristics of the Observed Sea Level Variability

The time series of observed sea level at all the tide gauge stations under consideration are depicted on the figure 3.4. As can be observed short time variations dominate at all stations with amplitudes ranging around ± 30 cm, as described previously by de Cuevas et al. (1986). The curves indicate that the variations of the daily mean sea levels are highly correlated. The figure illustrates also some seasonal variability at all stations although not highly pronounced. High sea level is observed in austral summer while low sea level is observed in the austral winter.

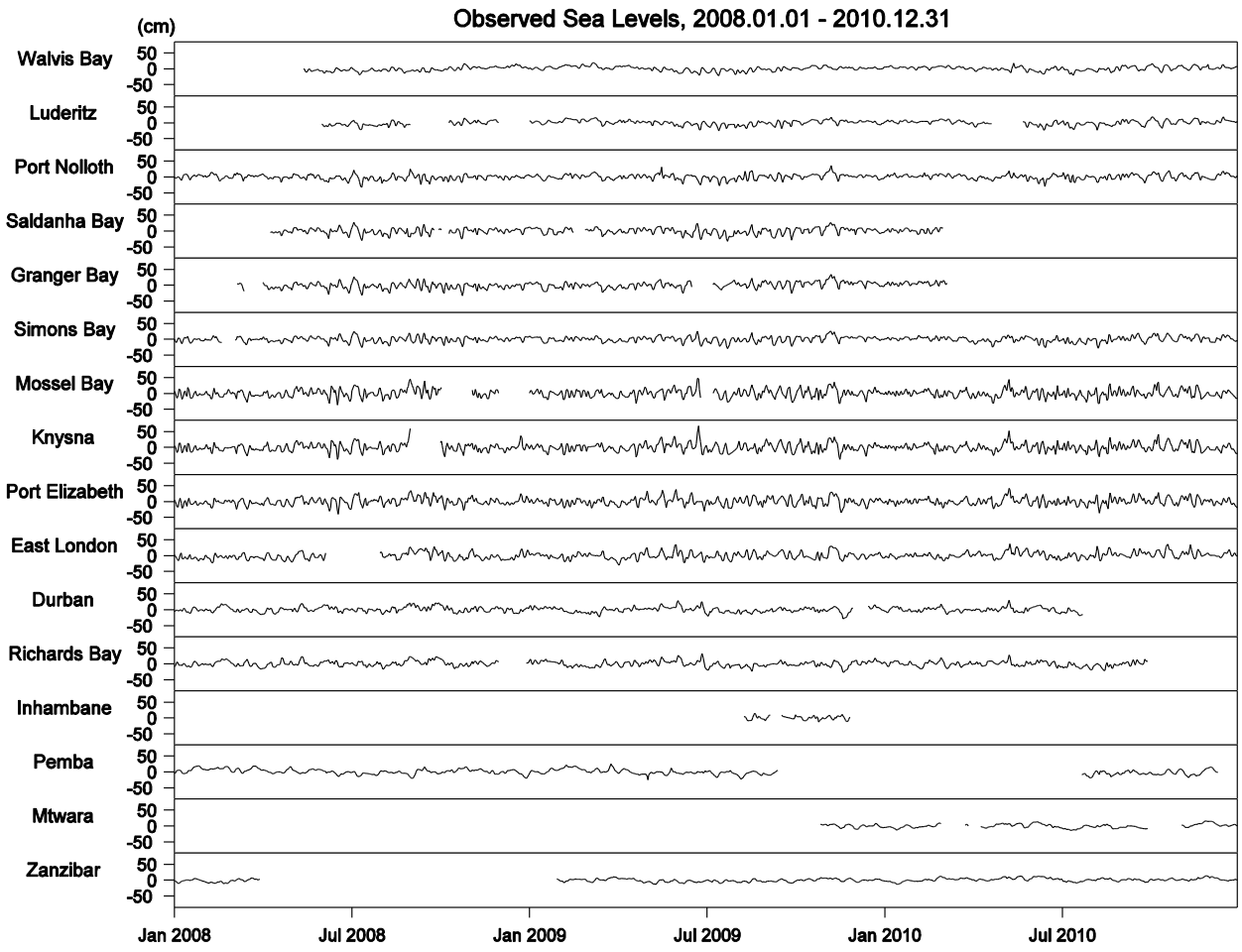


Figure 3. 4: Time series of the observed daily mean sea level variability around Southern Africa.

It may also be observed that the most pronounced deviations from the mean sea level occur most frequently along the west and south coasts of Southern Africa, roughly south of 27$^{o}$S. It means that in the northern part of Southern Africa, north of 27$^{o}$S, the sea level does not change too much from the mean. These deviations (figure 3.4) occur approximately two months before austral summer or winter corresponding to the spring or autumn in the southern hemisphere. From the time series of deviations (anomalies), several large events occurred around the coast of Southern Africa. The similarity in the amplitudes of individual events, at different coastal locations confirms results found by de Cuevas et al. (1986).

Figures 3.5 (a), (c) and (e) show the power density spectra at Port Nolloth, Simon's Bay and Port Elizabeth, respectively. On the power density spectra of Simon's Bay for example (figure

3.5 (c)) the time series typically showed a broad peak centred at a frequency of about 0.1 cycles per day, corresponding to the characteristic frequency of CTWs at Cape Town (e.g. de Cuevas et al., 1986; Schumann and Brink, 1990).

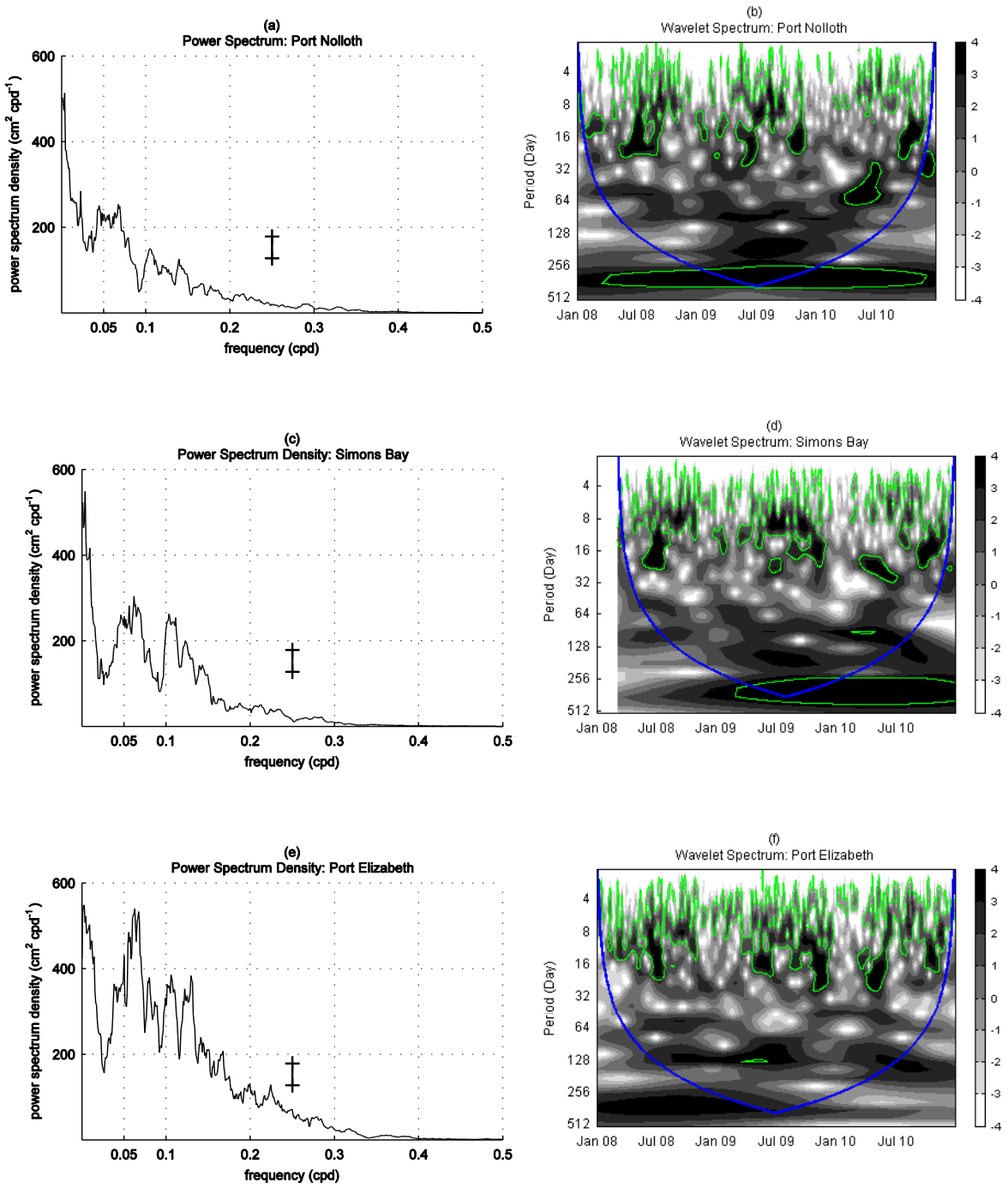


Figure 3.5: Power spectrum (a), (c) and (e) using the multi-taper method with adaptive weighting for the sea level variability at Port Nolloth, Simon's Bay and Port Elizabeth, respectively. 95% confidence (limit) plots are represented. Wavelet power spectrum (b), (d) and (f) for the sea level variability at Port Nolloth, Simon's Bay

and Port Elizabeth, respectively. Grey shades show the wavelet spectral power (units: base 2 logarithm of sea level variance). The green contour denotes the 95% significance level. Blue line is the cone of influence meaning that anything below is dubious.

The wavelet power spectrum at the same location was used to see the sea level variability from a time varying perspective, e.g. figure 3.5 (b, d, f). As can be seen short, term variability dominates during austral winter. The dominant modes of variability are not maintaining their shape year to year at each station point, reflecting variation in the inter-annual wind forcing.

To obtain an initial understanding of the wind forcing, figure 3.6 shows the standard deviation for the sea level and the alongshore wind variations. The standard deviation for the sea level shows three peaks, the highest one around Knysna on the south coast, the middle one around Granger Bay on the west coast and the lowest around Pemba on the east coast. The alongshore wind variations present two peaks around Luderitz and Saldanha Bay, respectively.

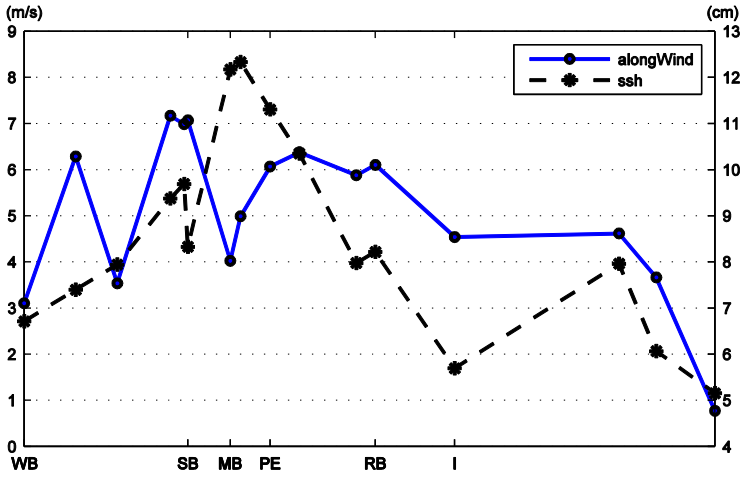


Figure 3.6: Standard deviations for the short term variations of the sea level (dashed curve in cm) and the alongshore wind (solid curve in m/s). The x-axis indicates the distance from Walvis Bay. Note that "WB", "SB", "MB", "PE", "RB", "P" and "Z" means Walvis Bay, Simon's Bay, Mossel Bay, Port Elizabeth, Richard's Bay, Pemba and Zanzibar, respectively.

The characteristics of the observed sea level variability were presented and the comparison done on the figure 3.6 is static. It does not give idea of how they really relate to each other. Therefore, using suitable techniques, the relationship between sea level and alongshore wind can be understood. This relationship between them in time or/and in space is explored in

section 4.3, below. By investigating the propagation of short term variability one objective of this study can be reached.

## 4.2 Characteristics of the Sea Level Variability from the Hybrid Coordinate Ocean Model (HYCOM)

Figure 3.7 shows the time series of the daily mean sea level variability from HYCOM at a grid point closest to all the tide gauge stations under consideration. The model daily output sea level height anomaly from the mean sea level is used to compare with the observed dataset anomaly. The mean sea surface heights were calculated for the period 1997 – 2007. As can be seen, short time variations dominate at all stations with amplitudes ranging around ± 30 cm. The curves at adjacent stations indicate that the variations of the daily mean sea levels are highly correlated. The figure illustrates also some seasonal variability at all stations, although this is not highly pronounced. High sea level is observed in austral summer while low sea level is observed in the austral winter.

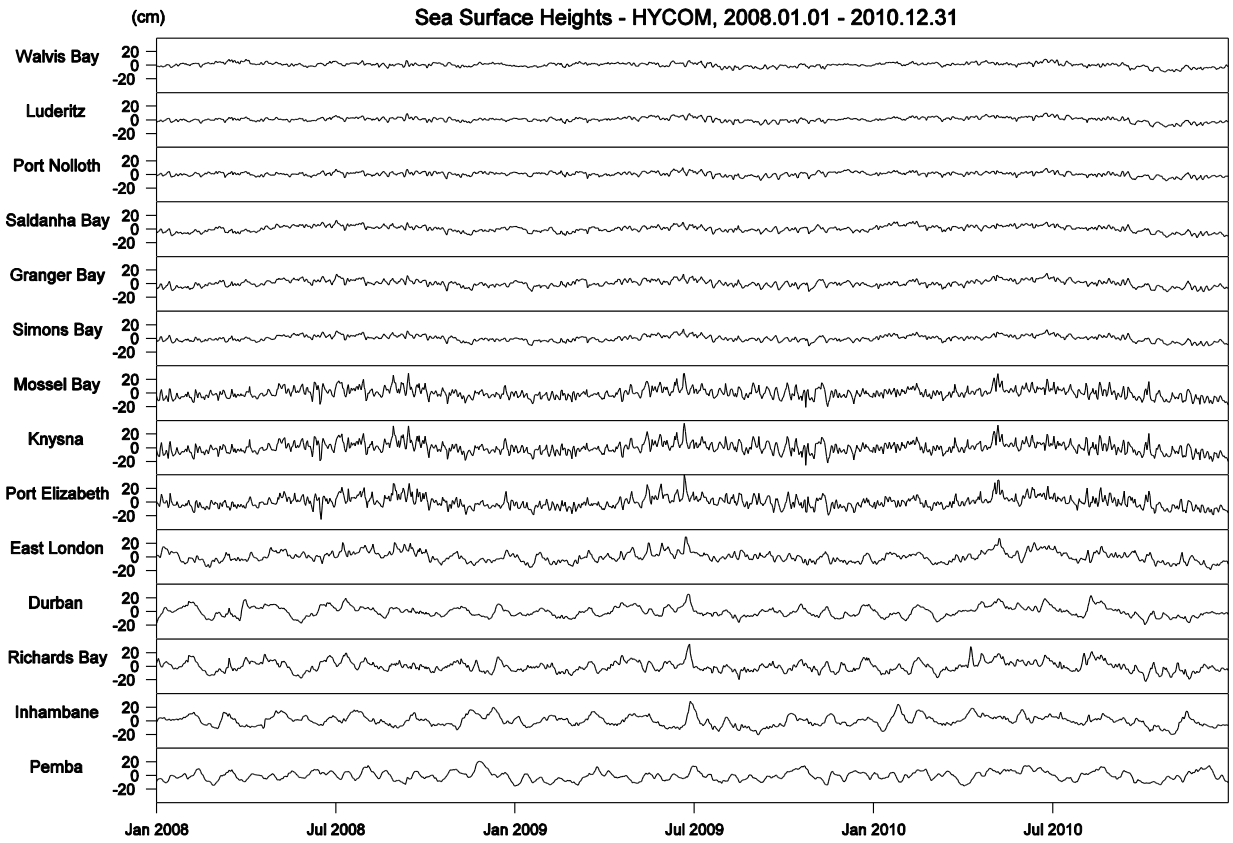


Figure 3.7: Time series of the daily mean sea level variability around Southern Africa from HYCOM.

In general, HYCOM model appears to be able to simulate both the spatial and temporal sea level variations well and with comparable amplitude to the in situ observations. However the scales used can induce to different visual conclusion so, for better understanding the comparison of the amplitude must be done station by station. In section 4.3, below, the relationship between sea level and alongshore wind in time or/and in space is explored to understand the propagation characteristics of the sea level variability's.

# 4.3 Propagation of short term variability

The Hovmöller diagrams were used to show the spatial-temporal distribution and evolution of the daily sea level anomaly. Figure 3.8 shows the Hovmöller diagrams for the same period of observed tide gauge anomalies and the model sea level data anomalies. Putting both diagrams

side-by-side allows a good comparison between them and to evaluate whether the model can reproduce the signals propagating around southern Africa.

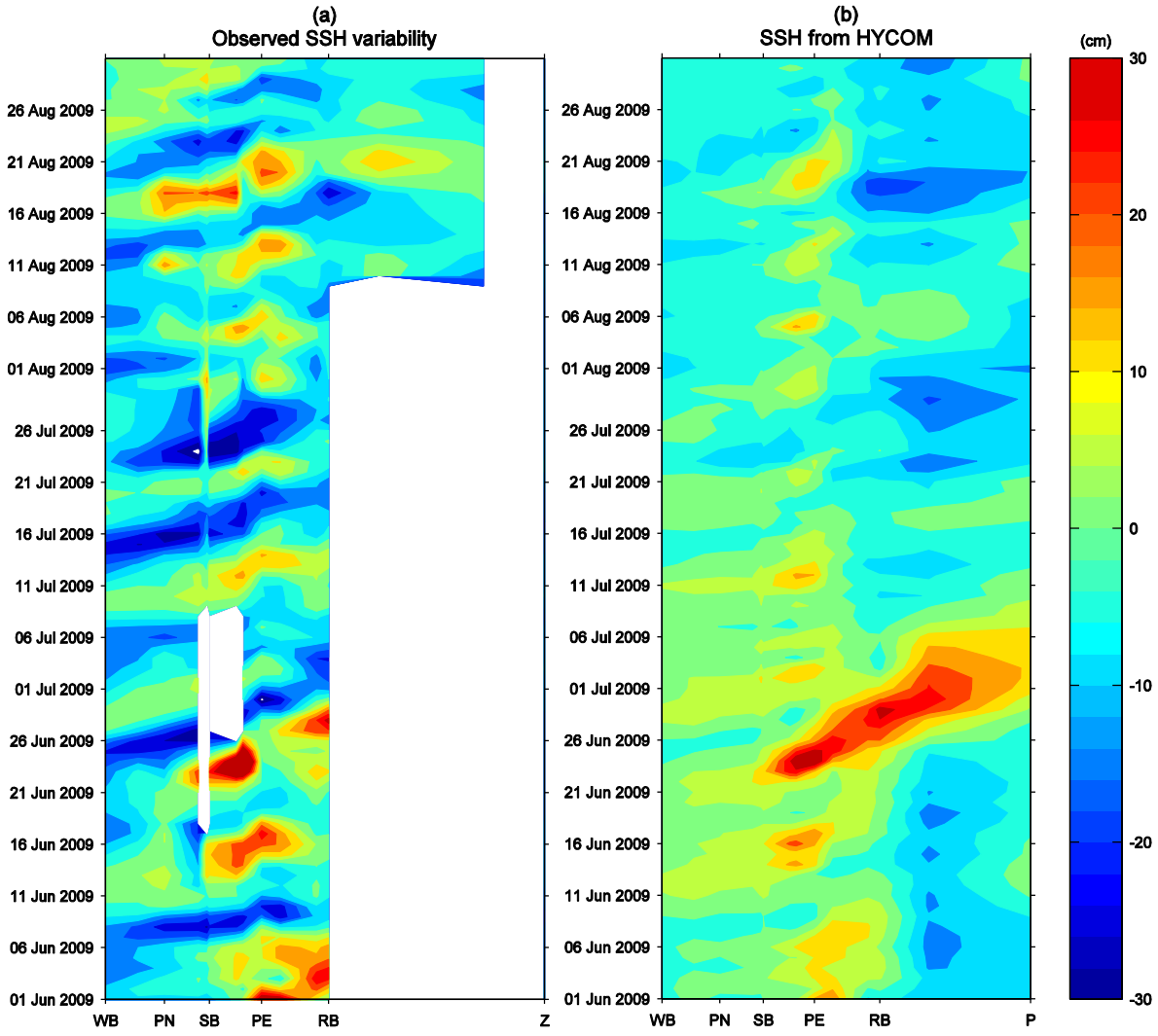


Figure 3.8: Hovmöller plot for (a) the observed sea level variability and (b) the sea level variability from HYCOM model from 01 June to 31 August, 2009. The x-axis represents the distance along the coast from Walvis Bay (WB) to Zanzibar (Z) for the tide gauges, and Pemba (P) for the model output. This spatial difference is due to the HYCOM model domain. White square indicate missing values.

It is clear that most of the events (both positive and negative), reach their maximum amplitude at the south coast between the Simon's Bay and Port Elizabeth, (SB and PE) on Figure 3.7. Due to lack of tide gauge data north of RB, it is not clear what happens to the observed anomalies to the north. From the model output, (Fig.3.8 b) the anomaly amplitudes clearly start to decay after PE. Only one extreme event (21 June 2009) travels as far north as Pemba

in Mozambique. This event will be studied in more detail below. Both positive and negative events can be seen, where the major events are negative but always proceeded by a positive disturbance; similar to what was found by de Cuevas et al. (1986).

Using the results of the lag correlation between sites, the disturbances take one to two days travelling southwards along the west coast (section from Port Nolloth-Simon's Bay) and one to six days travelling along the south coast (section from Simon's Bay-Port Elizabeth). The estimated propagation speed for the west coast appears to be fairly stable, ranging between 3 and 6.5 m/s. However, along the south coast, the estimated propagation speed ranges from 1 to 7.5 m/s.

As can be seen on the figure 3.8 (a), a strong event occurred from around 21 June to 02 July, 2009, which is well reproduced by the model on the figure 3.8 (b). In order to better understand the evolution of the sea level anomaly, plots of the wind stress together with the sea level pressure were produced. The daily sequence of plots of surface wind and pressure for the period 21 June-2 July 2009 is shown on Figure 3.9.

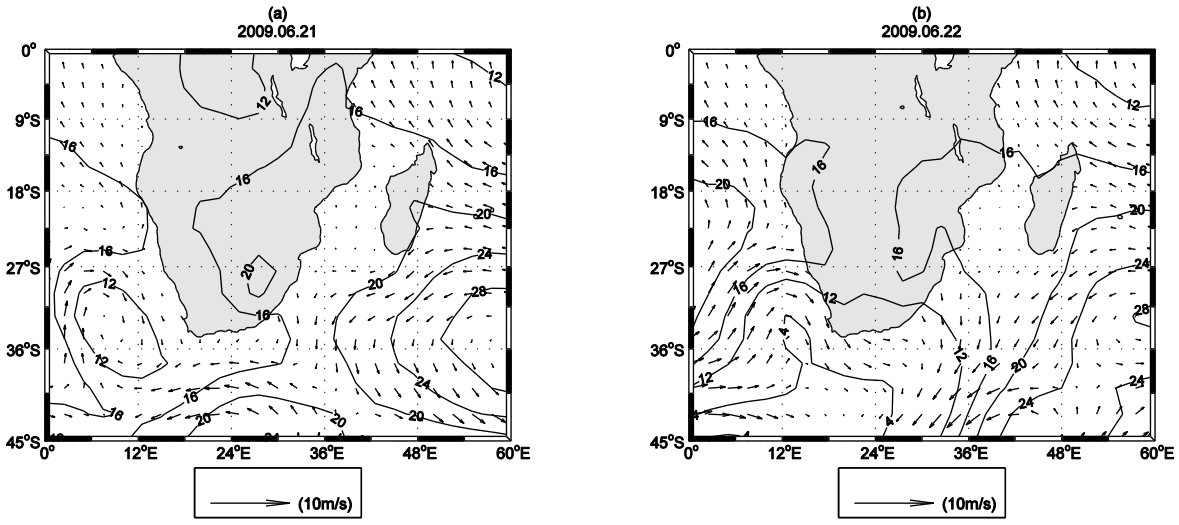

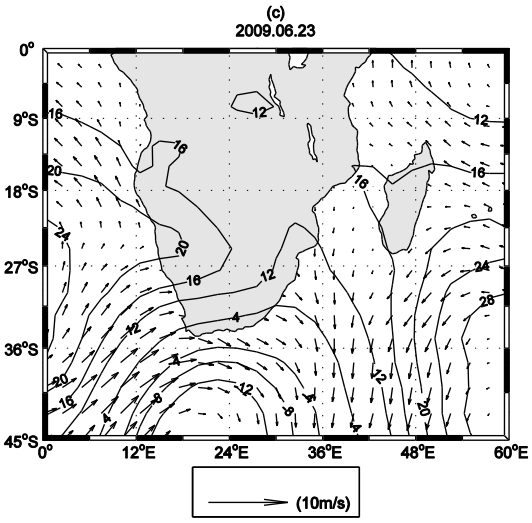
(c)
2009.06.23
0°
9°S
18°S
27°S
36°S
45°S
0°
12°E
24°E
36°E
48°E
60°E
(10m/s)

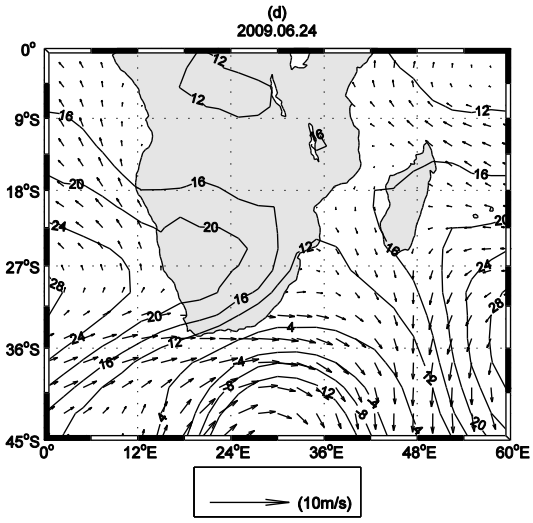
(d)
2009.06.24
0°
9°S
18°S
27°S
36°S
45°S
0°
12°E
24°E
36°E
48°E
60°E
(10m/s)

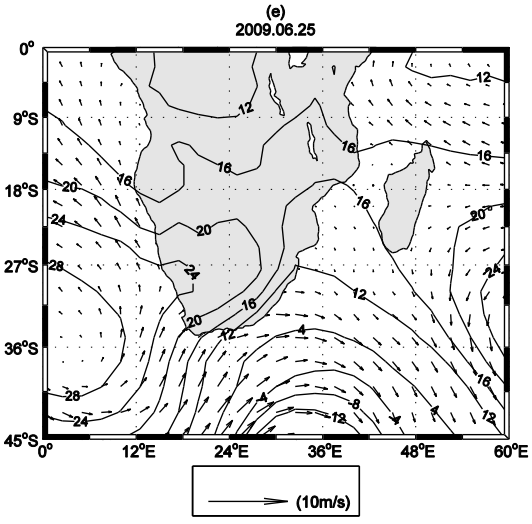
(e)
2009.06.25
0°
9°S
18°S
27°S
36°S
45°S
0°
12°E
24°E
36°E
48°E
60°E
(10m/s)

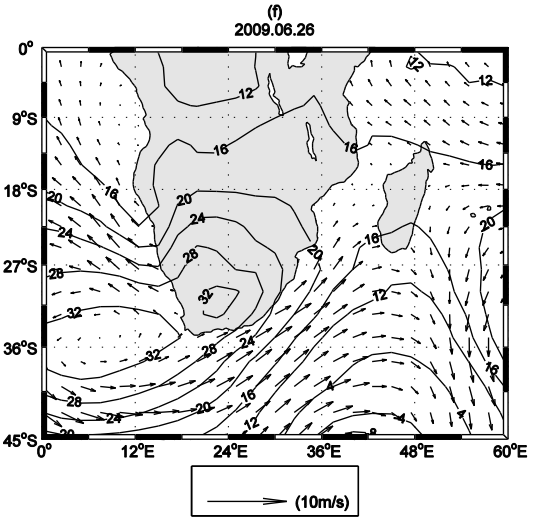
(f)
2009.06.26
0°
9°S
18°S
27°S
36°S
45°S
0°
12°E
24°E
36°E
48°E
60°E
(10m/s)

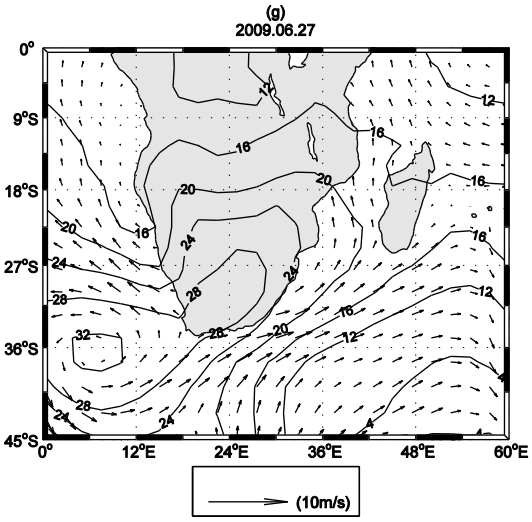
(g)
2009.06.27
0°
9°S
18°S
27°S
36°S
45°S
0°
12°E
24°E
36°E
48°E
60°E
(10m/s)

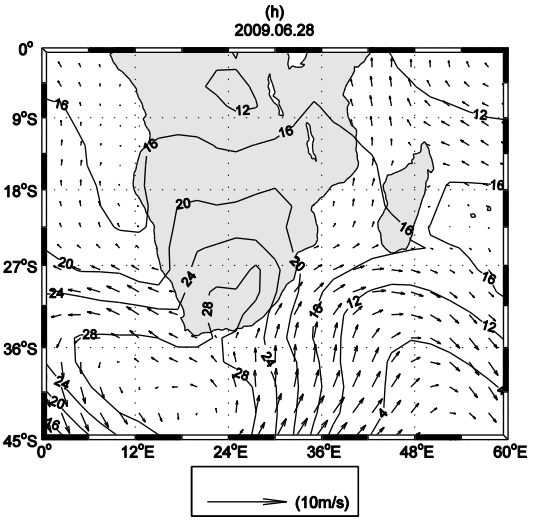
(h)
2009.06.28
0°
9°S
18°S
27°S
36°S
45°S
0°
12°E
24°E
36°E
48°E
60°E
(10m/s)

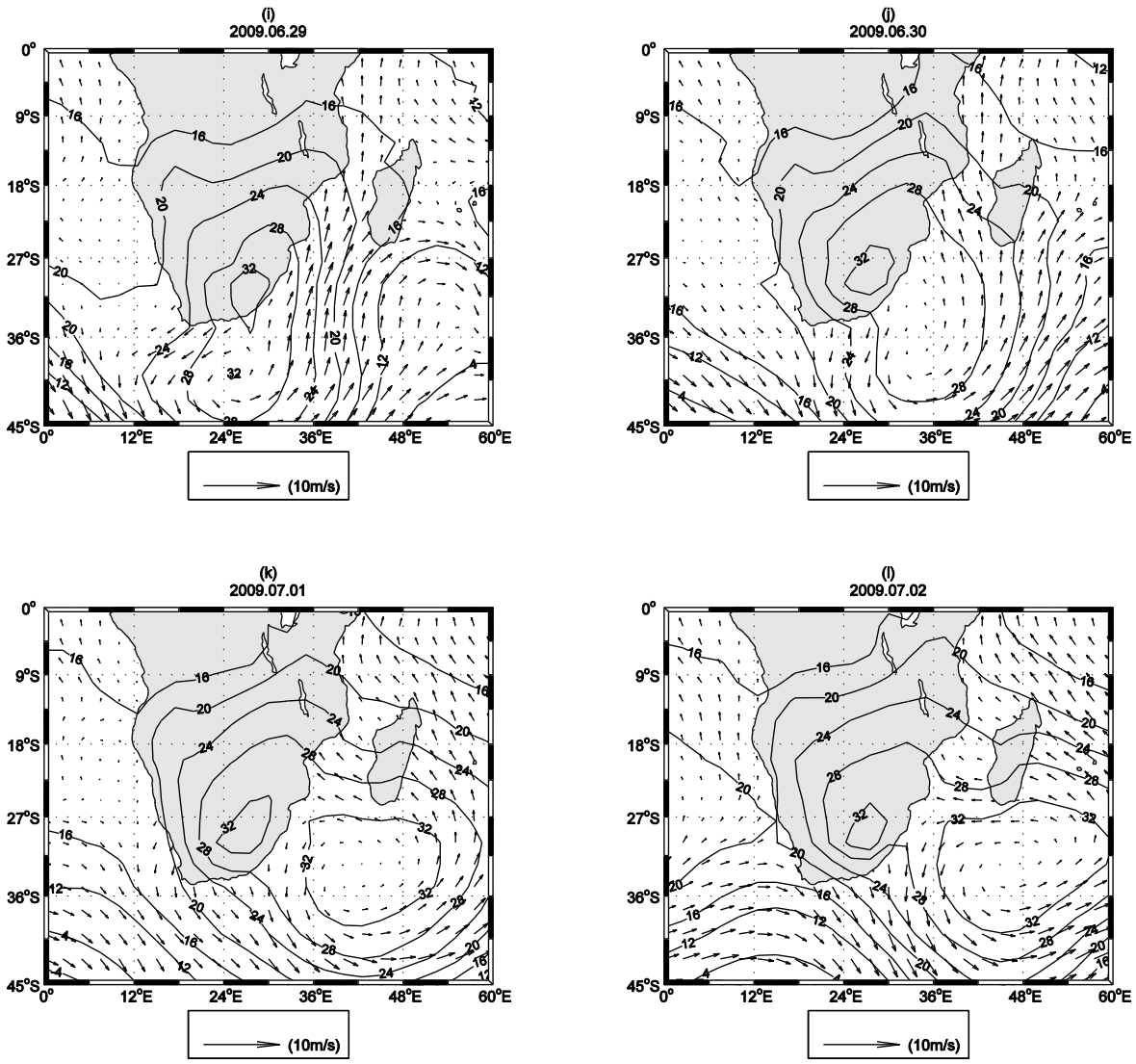


Figure 3.9: Sequence of daily wind vectors and sea level pressure (contour unit in $10^3$ Pa) around Southern Africa from 21June to 2 July 2009.

More details regarding the event aforementioned is done in the next chapter. Therefore, the analyses below explore and discuss the propagation characteristics of the sea levels around the coast of southern Africa and their association with the wind forcing, during this event.

# Chapter 5

# DISCUSSION

It was decided that a minimum of a three year period of good sequential air pressure adjusted tide gauge sea level anomaly data was necessary to investigate the nature and propagation of coastal trapped waves (CTWs) around southern Africa. Although there is scant sea level observation at stations like Inhambane, Mozambique, the decision to keep it for the study was important in order to give an idea of the CTWs evolution north of Richard's Bay station. There is clearly a risk that the northward propagating CTW may decay unobserved between Richard's Bay and Pemba. Another reason, perhaps less scientifically acceptable, is to subtly encourage the institutions responsible for setting up tide gauges in Mozambique to make a bigger effort to do so. It is of course known that this involves substantial infrastructure costs, and the technical capacity to maintain the instruments over long periods.

It seems that, in general, not all the stations respond isostatically. This apparent "non-isostatic" sea level variability has been motivated from a rather sparse network of tide gauges, the results of which could easily be misinterpreted. This lack of direct response to local atmospheric pressure forcing could mean that efforts must be given to understand the action of the wind on the sea level variability. In this way the inverted barometric correction was applied just to reduce the ''noise'' related to regional phenomena in the tide gauge data (e.g. Church et al., 2004).

The observations and results of the analyses show perturbations propagating anticlockwise with coastal trapped waves (CTWs) characteristics. The sea level perturbations start in many cases between Walvis Bay and Luderitz, Namibia. The amplitudes of the sea level variations caused by weather band processes range from 20-34 cm, from 22.5-53 cm and from 13.5-41 cm, along the west, south and east coast of southern Africa, respectively (see table 1). Krause and Radok (1976) and Schumann and Brink (1990) also found amplitudes greater than 50 cm off the south coast of Australia and southern Africa, respectively. The propagation of the

disturbances from the west coast to east coast is clear, although there are some events which appear not to be continuous from Port Nolloth to Simon's Bay. Schumann and Brink (1990) also reported propagation characteristics similar to this. As described by de Cuevas et al. (1986), there are differences in the frequency and activity of disturbances in winter and in summer, due to the differences in the nature of the weather systems forcing them. In this study, both station seasons show a lot of coherent events (figure 3.4). The beginning of both the summer and winter seasons appears to show strong disturbances.

In summer, the frequency and activity of the disturbances appear to be less intense when compared to the winter. The perturbations are due to strong and persistent south or south-easterly winds, as described in section 2.3, along the west coast. These perturbations, associated with upwelling events, are sufficiently strong to propagate as CTWs southwards down to the south coast of southern Africa. The amplitude of each coherent event appears to grow throughout its propagation until it disappears, usually near Port Elizabeth or East London.

In winter, the frequency and activity of the disturbances appear to be most intense, along the west coast from Port Nolloth and along the south coast of southern Africa. As was described in section 2.3, there is a lot of instability over these areas associated with the passage of the cold fronts from west to east. The weather systems linked to the cold front can be strong and persistent enough to generate and propagate CTWs along the south-east coast as far north as the Mozambique Channel. Because of high frequency of events, their amplitude seems similar. In general, at Walvis Bay and Luderitz and, at Durban and Richards Bay the amplitude is smaller.

The result of power density spectra (figures 3.5 (a), (c) and (e) and, appendix A) shows significant peaks for a period shorter than one month. It also confirms the analyses done by de Cuevas et al. (1986) and, Schumann and Brink (1990). Maiwa et al. (2009) also found similar results along the southern and eastern coasts of Australia. A relatively flat spectrum is shown at Port Nolloth with significant peaks around 7, 10 and 25 days, respectively. At Simon's Bay, although the significant peaks apparently maintain the same range as at Port Nolloth, they appear to be more developed. The spectrum at Port Elizabeth seems amplified although maintaining the same range of period as the two previous places. Here, although not

significant, there is some indication of the development of peaks before 7 days; Schumann and Brink (1990) reported similar behaviour at the same place. Just for notation, the spectrum at Knysna (see appendix A) is one that shows the wider 10 day peak than at the other tide stations. In general, the west coast (section Port Nolloth to Simon's Bay), and the south coast (section Simon's Bay to Port Elizabeth) shows diverse significant spectral peaks with periods ranging from about 7 to 25 days, respectively. The east coast, actually the south-east coast (section East London to Richard's Bay) shows flat spectra dominated by longer period energy around 25 days; Schumann and Brink (1990) related this pattern to variations in the Agulhas Current.

The wavelet power spectrum (figures 3.5 (b), (d) and (f) and, appendix A) demonstrates that frequency and activity of the disturbances is intense, as above mentioned. It is proved by the large amplitude during austral winter of the short term variability; the analysis of Maiwa et al. (2009) reported similar results along the southern and eastern coasts of Australia. At Port Nolloth, the dominant modes of CTW activity are highly variable and gradually lengthen from 7 days in 2008 to around 60 days in 2010. The dominant modes at Simon's Bay tend to be uniform and lengthen from 10 days in 2008 to around 30 days in 2010. At this tide gauge, the activity of the disturbances can clearly be distinguished between summer or winter. At Port Elizabeth, the dominant modes of variability are consistent and persistent. Apparently, the frequency and the activity of the disturbances in both summer and winter season have very small differences. The dominant period and the amplitude of the variability are variable from year to year at each station point (see figures 3.5 (b), (d) and (f) and, appendix A). In the west coast (section Port Nolloth to Simon's Bay) and in the south coast (section Simon's Bay to Port Elizabeth) the dominant modes of variability gradually lengthen from 7 days in 2008 to around 60 days in 2010.

The relationship between the sea level height and the wind forcing (figure 3.6) is shown using their standard deviation. The standard deviation for the sea level shows three peaks, the highest one around Knysna in the south coast, the middle one around Granger Bay near Cape Town on the west coast and the lowest around Pemba (Mozambique) on the east coast. The alongshore wind variations present two peaks around Luderitz and Saldanha Bay, respectively. This shows that, along the west coast of southern Africa, two wind systems or

subsystems dominate, one terminating around at Port Nolloth another commencing around at same place. The wind system that appears to commence there has it peak near Saldanha Bay. Thus in the section Port Nolloth to Mossel Bay the sea level seems to be continuously forced by the wind and it seems that the sea level variability can propagate as coastal trapped waves further to the south. Another peak of wind variability not pronounced near East London can be associated with the large sea level variation along the south coast.

The daily mean sea level heights from the Hybrid Coordinate Ocean Model (HYCOM), in general, present perturbations propagating anticlockwise with coastal trapped waves (CTWs) characteristics (figure 3.7). Unfortunately the model does not reproduce the variability along the west coast very well. Apparently it is in term of magnitude of sea level variability because it seems to have a shape similar to sea level variability from the observed data. While it seems to underestimate the response on the west coast, at same time it seems to overestimate the CTW response along the east coast of southern Africa.

The comparison of both observed and HYCOM model outputs sea levels can be made by analyzing the Hovmöller diagrams (figures 3.8 and appendix B). Firstly, the signal does not always propagate all the way from the west to the east coast of southern Africa (figure 3.8 and appendix B). The amplitude of some propagating signals strengthens in the east coast (between the locations denoted “PE” and “RB” in the horizontal axis in figure 3.8(a)), while some of them are observed only in a limited area in the south region, and some are drastically weakened or even disappear after passing the location between Port Elizabeth and East London in the east coast of southern Africa. The figures suggest that the disturbance presented by HYCOM outputs matches with those find on the observed data (see figures 3.8 and appendix B). In other words, there is a good agreement between observed and modelled CTW activity along the east coast, especially where such disturbances are infrequent and difficult to find in the observed data. The aforementioned area is mostly dominated by meso-scale eddies (e.g. Gründlingh, 1983; Sætre and da Silva, 1984; Biastoch and Krauss, 1999; de Ruijter et al., 1999; de Ruijter et al., 2002) which can generate short time perturbations (Louis, 1989). The figures also suggest that the west is actually the starting point for the disturbances (see figures 3.8 and appendix B). In this case, the starting point is the area between Walvis Bay and

Luderitz, because of the lack of observed data to prove otherwise (e.g. further north in Angola).

The results from the lag correlation gave a typical period of propagation of the disturbances along the west (section Port Nolloth-Simon's Bay) and the south coast (section Simon's Bay-Port Elizabeth) is one to two days and one to six days, respectively. The estimated propagation speed for the west coast ranges between 3 and 6.5 m/s, while in the south coast, is from 1 to 7.5 m/s, also from the lag correlation. This suggests that with a narrow shelf width/slope the coastal trapped waves move faster than where the distance from the coast to the shelf slope is greater (see figure 3.1). But, it can also be the effect of a continuously forcing agent resulting in sea level variability propagating as coastal waves; de Cuevas et al. (1986) suggested the second reason.

The sequence of daily wind vectors and sea level pressure (figure 3.9) around the coast of southern Africa from around 21 June to 02 July, 2009, is an example of the relation between the two variables during the generation and eastward propagation moments. On 21 June (figure 3.9 (a)), a low pressure system is located near the south-western corner of southern Africa, centred at about 35°S, 10°E, with northerly winds along the west coast. At the same time, easterly winds along the south coast are observed due to the high pressure system with its core centred far south. These winds tend to generate positive sea level anomaly (SLA) along the west coast and a negative signal along the east coast, respectively (see also figure 3.8 (b)). Maiwa et al. (2009) analysed similar features, around the southern and eastern coasts of Australia, which generated results rather different from these. They found significant strong northerly winds along the western coast of Australia when a low-pressure system was located near the southwestern corner of Australia, centered at 32°S, 109°E. The difference is perhaps due to the fact that the length of the southern coast of Australia is greater compared to that of the south coast of southern Africa. In addition, it could be due to the fact that the southern coast of Australia is located at a latitude further south than the south coast of southern Africa. As result, off Australia, the cores of both low and high pressure systems are nearest the southern coast.

As can be noted on the figure 3.9 (b) strong northerly winds prevailed along the west coast on 22 June 2009, simultaneously with the displacement of the low pressure system eastward. By 24 June, the Atlantic high pressure system propagates eastward starting to influence the west coast, while the low pressure system is forced move eastward down south along the subcontinent (figure 3.9 (d)). This causes southerly winds along the west coast and strong westerly winds along the south coast. The result is the negative sea level anomaly along the west coast and a positive signal in the south and southeast coast, respectively. (Note that an amplitude of about 53 cm was recorded at Knysna, in the middle of the south coast). The high pressure system reached the continent and broke into two cores: one centred at 36°S, 06°E another one centred at 30°S, 23°E (on the continent) on 26 June, with westerly winds prevailing over the south eastern part of southern Africa. By 29 June, the high pressure system is still over the continent but moves eastward to 30°S, 27°E with strong southerly winds along the east coast. At this time, the winds along the east region of the coast of southern Africa are favourable for the positive sea level anomaly signal. The high pressure system in the atmosphere strengthens and remains around the same location by 30 June, enhancing positive and generating negative SLA in the northern and, in the southern part of the eastern coast of southern Africa, respectively. By 02 July 2009, there are wind divergences in the western region and near the south-western corner of Mozambique Channel; the result is a negative sea level anomaly. Unfortunately it cannot be entirely confirmed on figure 3.8 (a), but only along the west coast, due to missing tide gauge data along the east coast.

Analyzing the frequency and activity of the disturbances, before mentioned, let us have a look to the figure 3.1. The figure shows the bathymetry of the coastal shelf region of southern Africa. The frequency and activity of the coastal trapped waves appears to be so intense on the section Mossel Bay-East London. It seems to be associated the wide and shallow sloping bottom on the Agulhas Bank, south of Africa. Thus, it can be said that there is a relationship of proportionality between the width of the coast shelf and propagation speed of CTWs. If there is such a relation, what is cause/effect of the relationship? This can probably be motivated by a “funneling” of the shelf. So, when CTWs are spreading slowly “enjoying” the good conditions for their survival along the southern coast, the shelf begins an almost uniform narrowing taper to the east near $32^{o}$ S and $22^{o}$ E. The CTWs appear to be accelerated before they reach this section.

The results suggest that the CTWs propagate as forced coastal trapped waves. This propagation characteristic has an effect on their behaviour from Port Elizabeth to the equator. The CTWs can travel northwards against the very strong Agulhas Current, only when a very strong and favourable weather system such as discussed on the figure 3.9 is the forcing behind the disturbance. These results suggest that the stronger and more persistent the weather system is, the more likely it is to resonate with the coastal trapped wave. The speed of propagation is governed by the shelf characteristics, and if the travelling wind system matches this speed, the CTW amplitude is likely to grow.

# Chapter 6

# CONCLUSIONS

The propagation characteristics of the coastal trapped waves (CTWs) around the coast of southern Africa have been investigated by analyzing the observed daily mean sea level data from coastal tide gauges, as well as daily sea level anomalies outputs from the Hybrid Coordinate Ocean Model (HYCOM). The findings of this research are now summarized and judge the success or otherwise according to the aim and the first research question posed in the beginning:

i. Can the coastal trapped waves propagate equatorward along the east coast of southern Africa in the opposite direction of the Agulhas current?

The observed sea level variability around the coast of southern Africa is dominated by the short time variability with a period shorter than one month. The short time variability varies from season to season with the largest CTW amplitude during austral winter. The short time variability propagates anticlockwise around the coast of southern Africa with a propagation speed ranging from 3 to 6.5 m/s, and from 1 to 7.5 m/s, along the west and south coasts, respectively. These propagation speeds are forced by synoptic atmospheric disturbances mainly in term of wind variability.

Coastal trapped waves were observed to propagate equatorward on the east coast of southern Africa in the opposite direction of Agulhas current on a few occasions. It can be determined by a good resonant forcing between a strong and persistent weather system and the coastal trapped wave.

Longer time records from Inhambane and better use of model outputs would help to get more precise response and bring good answers for some discrepancies that were found. Concerning the second question:

ii. Can the Hybrid Coordinate Ocean Model (HYCOM) output of sea level anomalies, for southern Africa, reproduce the coastal trapped wave's signal of the tide gauges?

The outputs from Hybrid Coordinate Ocean Model (HYCOM) show very similar propagation characteristics to the observed data. Along the south coast, the behaviour of the CTW is well reproduced. Unfortunately the model does not reproduce very well the variability along the west coast. While it seems to underestimate the west coast response, at same time it seems to overestimate it along the south coast of southern Africa. Although the model demonstrated some CTWs travelling northwards along the east coast, such disturbances were infrequent and difficult to find in the observed data. The infrequence and difficult aforementioned is motivated by gaps on the data of the tide gauges located on the east coast.

There is a need to develop a better and profound understanding of the CTW behaviour on the east coast of southern Africa. Long tide gauge records, mainly in the east coast, are required and will continue to play a major role together with model data in determining the aforementioned understanding. A preliminary assessment of the model outputs around the coast of southern Africa must be done. In addition is a need to improve the model outputs in the west coast for eliminating the under-estimation found. This will allow an accurate conclusion whether the CTWs can propagate northward along the east coast of southern Africa. Techniques such as space and time-lagged correlation also must be explored, mainly using observed sea level variability and alongshore wind, to get more accurate answer.

# Bibliography

Adams, J. K. and V. T. Buchwald (1969): The Generation of Continental Shelf Waves. *J. Fluid Mech.*, **35**, 815 – 826.

Antonov, J. I., R. A. Locarnini, T. P. Boyer, A. V. Mishonov and H. E. Garcia (2006): World Ocean Atlas 2005, Volume 1: Salinity. *NOAA Atlas NESDIS,* **61**, U.S. Government Printing Office, Washington, 182 pp.

Antunes, C. and R. Taborda (2011): Sea Level at Cascais Tide Gauge: Data, Analysis and Results. *J. of Coastal Research*, SI **56** (Proceedings of the 10th International Coastal Symposium), 218 – 222. Lisbon, Portugal, ISSN 0749-0258.

Antunes, C. (2011): Monitoring sea level change at Cascais tide gauge. *J. of Coastal Research*, SI **64** (Proceedings of the 11th International Coastal Symposium), 870 – 874. Szczecin, Poland, ISSN 0749-0208.

Backeberg, B. C., J. A. Johannessen, L. Bertino and C. J. Reason (2008): The greater Agulhas Current system: An integrated study ofits mesoscale variability. *J. Op. Oceanogr.* **1** (1), 29 – 44.

Backeberg, B. C. (2009): Modelling the mesoscale variability in the greater Agulhas Current System using a Hybrid Coordinate Ocean Model. *PhD thesis,* University of Cape Town, South Africa.

Backeberg, B. C., F. Counillon and J. A. Johannessen (in press): Assimilating Along-track SLA data using the EnOI in an Eddy Resolving Model of the Agulhas System. 1 – 20.

Bentsen, M., G. Evensen, H. Drange, A. D. Jenkins (1999): Coordinate Transformation on a Sphere using Conformal Mapping. *Mon. Weather Rev.*, **127**, 2733 – 2740.

Biastoch, A. and W. Krauss (1999): The Role of Mesoscale Eddies in the Source Regions of the Agulhas Current. *J. Phys. Oceanogr.*, **29**, 2303 – 2317.

Bleck, R. (2002): An oceanic general circulation model framed in hybrid isopycnic-Cartesian coordinates. *Ocean Modelling* , **37**, 55 – 88.

Brink, K. H. (1990): On the Damping of Free Coastal-Trapped waves. *J. Phys. Oceanogr.*, **14**, 1079 – 1094.

Brundrit, G. B. (1981): Memorandum on a Research Proposal Pertaining to Low Frequency Sea Level Fluctuations off the South Africa. *Dep. of Phys. Ocean.*, UCT, 1 – 5.

Brundrit, G. B. (1984). Monthly mean sea level variability along the west coast of southern Africa. *S. Afr. J. Mar. Sci*, **2**, 195 – 203.

Brundrit, G. B. (1995): Trends of southern African sea level: statistical analysis and interpretation. *S. Afr. J. Mar. Sci*, **16**, 9 – 17.

Buchwald, V. and J. Adams (1968): The Propagation of Continental Shelf Waves, Proc. Roy. Soc., Ser. A, **305**, 235 - 250.

Chelton, D. B. , R. A. de Szoeke, M. G. Schlax, K. E. Naggar and N. Siwertz (1998): Geographical Variability of the First Baroclinic Rossby Radius of Deformation. *J. Phys. Oceanogr.*, **28**, 433 – 460.

Church*, J.* A., N. J. White, R. Coleman, K. Lambeck and J. X. Mitrovica (2004): Estimates of the Regional Distribution of Sea Level Rise over the 1950–2000 Period. *J. of Climate*, **17**, 2609 – 2625.

Church, J. A., N. J. White, T. Aarup, W. S. Wilson, P. L. Woodworth, C. M. Domingues, J. R. Hunter and K. Lambeck (2008): Understanding Global Sea Levels: Past, Present and Future. *Sustain Sci.*, 3, 9 – 22. DOI 10.1007/s11625-008-0042-4.

Dee, D. P., S. M. Uppala, A. J. Simmons, P. Berrisford, P. Poli, S. Kobayashi, U. Andrae, M. A. Balmaseda, G. Balsamo, P. Bauer, P. Bechtold, A. C. M. Beljaars, L. van de

Berg, J. Bidlot, N. Bormann, C. Delsol, R. Dragani, M. Fuentes, A. J. Geer, L. Haimberger, S. B. Healy, H. Hersbach, E. V. Hlm, L. Isaksen, P. Kllberg, M. Khler, M. Matricardi, A. P. McNally, B. M. Monge-Sanz, J. J. Morcrette, B. K. Park, C. Peubey, P. de Rosnay, C. Tavolato, J. N. Thpaut and F. Vitart (2011): The ERA-Interim reanalysis: Configuration and Performance of the Data Assimilation System. *Quar. J. of the Roy. Meteorol. Soc.*, **137**, 553 - 597. DOI 10.1002/qj.828. URL http://dx.doi.org/10.1002/qj.828

de Cuevas, B. A., G. B. Brundrit and A. M. Shipley, 1986: Low-frequency sea-level fluctuations along the coasts of Namibia and South Africa. *Geophys. J. R. asrr. Soc.,* **87**, 33 - 42.

de Ruijter, W.P.M., P. J. van Leeuwen and J. R. E. Lutjeharms (1999): Generation and evolution of Natal Pulses: Solitary Meanders in the Agulhas Current. *J. Phys. Oceanogr.*, **29**, 3043 – 3055.

de Ruijter, W. P. M., H. Ridderinkhof, J. R. E. Lutjeharms, M. W. Schouten and C. Veth (2002): Observations of the Flow in the Mozambique Channel. *Geophys. Res. Lett.*, **29**, 1502 – 1504.

de Ruijter, W. P. M., H. M. van Aken, E. Beier, J. R. E. Lutjeharms, R. P. Matano and M. W. Schouten (2004): Eddies and Dipoles around South Madagascar: Formation, Pathways and Large-scale Impact. *Deep-Sea Res.*, **51**, 383 – 400.

Duncan, C. P. (1970): The Agulhas Current. *PhD thesis*, University of Hawaii, Honolulu.

Emery W. J. and R. E. Thomson (2004): Data Analysis Methods in Physical Oceanography. *ELSEIVIER*, 2nd and rev. edn..

George, M.S., L. Bertino, O. M. Johannessen and A. Samuelsen (2010): Validation of a Hybrid Coordinate Ocean Model for the Indian Ocean. *J. Op. Oceanogr*. **3**(2), 25 – 38.

Gill, A. E. and A. J. Clarke (1974): Wind-induced upwelling, coastal currents and sea-level changes. *Deep-Sea Res*., **21**, 325–345.

Gill, A. E. and E. H. Schumann (1974): The Generation of Long Shelf Waves by Wind. *J. Phys. Oceanogr.*, **4**, 83 – 90.

Gill, A. E. and E. H. Schumann (1979): Topographically Induced Changes in the Structure of an Inertial Coastal Jet: Application to the Agulhas Current. *J. Phys. Oceanogr*., **9**, 975 – 991.

Gründlingh, M. L. (1983): On the course of the Agulhas Current. *S. Afr. Geograph. J.*, **65**, 49 – 57.

Hamon, B. V., 1962: The spectrums of mean sea level at Sydney, Coff's Harbour, and Lord Howe Island. *J. Geophys. Res.*, **67**, 5147 – 5155.

Hamon, B. V. (1966): Continental shelf waves and the effects of atmospheric pressure and wind stress on sea level. *J. Geophys. Res*., **71**, 2883–2893.

Hodnesdal, H. (2006): Test of 30-sec sampling of water level and decimating to 10-min data. Norwegian Hydrographic Service, IV.2.7.2-1, 1 – 34.

Hughes, T. (1992): The Impacts of Sea Level Rise on the South African Coastal Environment. *PhD thesis,* University of Cape Town, South Africa.

Huthnance, J. M. (1995): Circulation, exchange and water masses at the ocean margin: the role of physical processes at the shelf edge. *Prog. Oceanogr.*, **35**, 353 – 431.

IOC (1985): Manual on Sea Level Measurement and Interpretation: Volume I - Basic Procedures. Intergovernmental Oceanographic Commission, Manuals and Guides **14**, 1 – 78.

Krause, G. and R. Radok (1976): Long Waves on the Southern Ocean. *Waves in Water of Variable Depth*, D. G. Provis, R. Radok, Eds., Springer-Verlag, 221 – 231.

LeBlond, P. H. and L. A. Mysak (1978): Waves in the Ocean. Elsevier, 602 pp.

Locarnini, R. A., A. V. Mishonov, J. I. Antonov, T. P. Boyerand and H. E. Garcia (2006): World Ocean Atlas 2005, Volume 1: Temperature. *NOAA Atlas NESDIS*, **61**, U.S. Government Printing Office, Washington, 182 pp.

Louis, J. P. (1989): Current-shelf interactions during the Australian Coastal Experiment. *Aust. J. Mar. Freshwater Res*., **40**, 571 – 585.

Maiwa K., Y. Masumoto and T. Yamagata (2009): Characteristics of Coastal Trapped Waves along the Southern and Eastern Coasts of Australia. *J. of Oceanogr.*, **66**, 243 – 258.

Mather A. A. (2007): Linear and nonlinear sea-level changes at Durban, South Africa. *S. Afr. J. Sci.,* **103**, 509 – 512.

Miller, L. and B. C. Douglas (2004): Mass and Volume Contributions to 20th-Century Global Sea Level Rise. *Nature*, **428**, 406 – 409. doi: 10.1038/nature02309.

Mysak, L. A. (1967): On the theory of continental shelf waves off Oregon. *J. Marine Res*., **25**, 205 – 227.

Mysak, L. A. (1980): Recent Advances in Shelf Wave Dynamics. *Rev. of Geophys.*, **18**, 211 – 241.

Nelson, G. and L. Hutchings (1983): The Benguela upwelling system, *Prog. Oceanogr.*, **12**, 333 – 356.

Oki, T. and Y.C. Sud (1998): Design of the Global River Channel Network for Total Runoff Integrating Pathways (TRIP). *Earth Interactions*, **2**, 1 – 37.

Percival D. B. and A. T. Walden (1993): Spectral Analysis for Physical Applications - Multitaper and Conventional Univariate Techniques. *Cambridge University Press*, 612 pp.

Preston-Whyte, R. A. and P. D. Tyson (1988): The Atmosphere and Weather of Southern Africa. *Oxford University Press – South Africa*, 374 pp.

Pugh, D. T. (1987): Tides, Surges and Mean Sea-Level. *John Wiley & Sons*, 472 pp.

Reynaud, T., R. G. Ingram, H. J. Freeland and A. J. Weaver (1991): Propagation of Coastal Trapped Waves under an Ice Cover in Hudson Bay. *$C^2$GCR*, 91-7, 1 – 46.

Robinson, A. R. (1964): Continental shelf waves and response of sea level to weather systems. *J. Geophys. Res*., **69**, 367 – 368.

Sætre, R. and A. J. da Silva (1984): The circulation of the Mozambique Channel. *Deep-Sea Res.*, **31**, 485 – 508.

Schumann, E. H. (1983): Long-period Coastal Trapped Waves off the south-east coast of southern Africa. *Contin. Shelf Res.*, **2**, 97 – 107.

Schumann, E.H. (2013): Sea Level Variability in South African Estuaries. *S Afr J Sci*. 2013;109(3/4), Art. #1332, 7 pages. http://dx.doi.org/10.1590/sajs.2013/1332

Schumann, E. H. and K. H. Brink (1990): Coastal-Trapped Waves off the Coast of South Africa: Generation, Propagation and Current Structures. *J. of Phys. Oceanogr.*, **20**, 1206 – 1218.

Siedler, G., M. Rouault and J. R. E. Lutjeharms (2006): Structure and Origin of the Subtropical South Indian Ocean Countercurrent. *Geophys. Res. Lett.*, **33**, L24609, doi:10.1029/2006GL027399.

Taljaard, J. J. (1972): Synoptic meteorology of the Southern Hemisphere, In: Meteorology of the Southern Hemisphere, *Meteorol. Monogr. of the Am. Meteorol. SOC.*, **13**, N$^o$ 35, 139 – 213.

Thomson, W. (1879): On gravitational oscillations of rotating water. *Proc. Roy. Soc. Edinburgh*, **10**, 92.

Tomczak, M. (1998): Shelf and Coastal Oceanography. (**http://www.es.flinders.edu.au/~mattom/ShelfCoast/index.html**) 24/11/2013

Torrence, C. and G. P. Compo (1998): A Practical Guide to Wavelet Analysis. Bull. Am. Meteorol. Soc., **79**, 61 – 78.

Tyson, P. D. and R. A. Preston-Whyte (2000): The Weather and Climate of Southern Africa . *Oxford University Press – Incorporated*, 396 pp.

van Loon, H. (1972): Wind in the Southern Hemisphere, In: Meteorology of the Southern Hemisphere, *Meteorol. Monogr. of the Am. Meteorol. SOC.*, **13**, N$^{o}$ 35, 87 – 100.

Wallcraft, A. J., E.J. Metzger and S.N. Carroll (2009): Software Design Description for the Hybrid Coordinate Ocean Model (HYCOM) Version 2.2. Technical Report NRL/MR/7320--09-9166, Naval Research Laboratory.

# APPENDICES

## A. Power spectrum density and wavelet power spectrum for the sea level variability at each tide station.

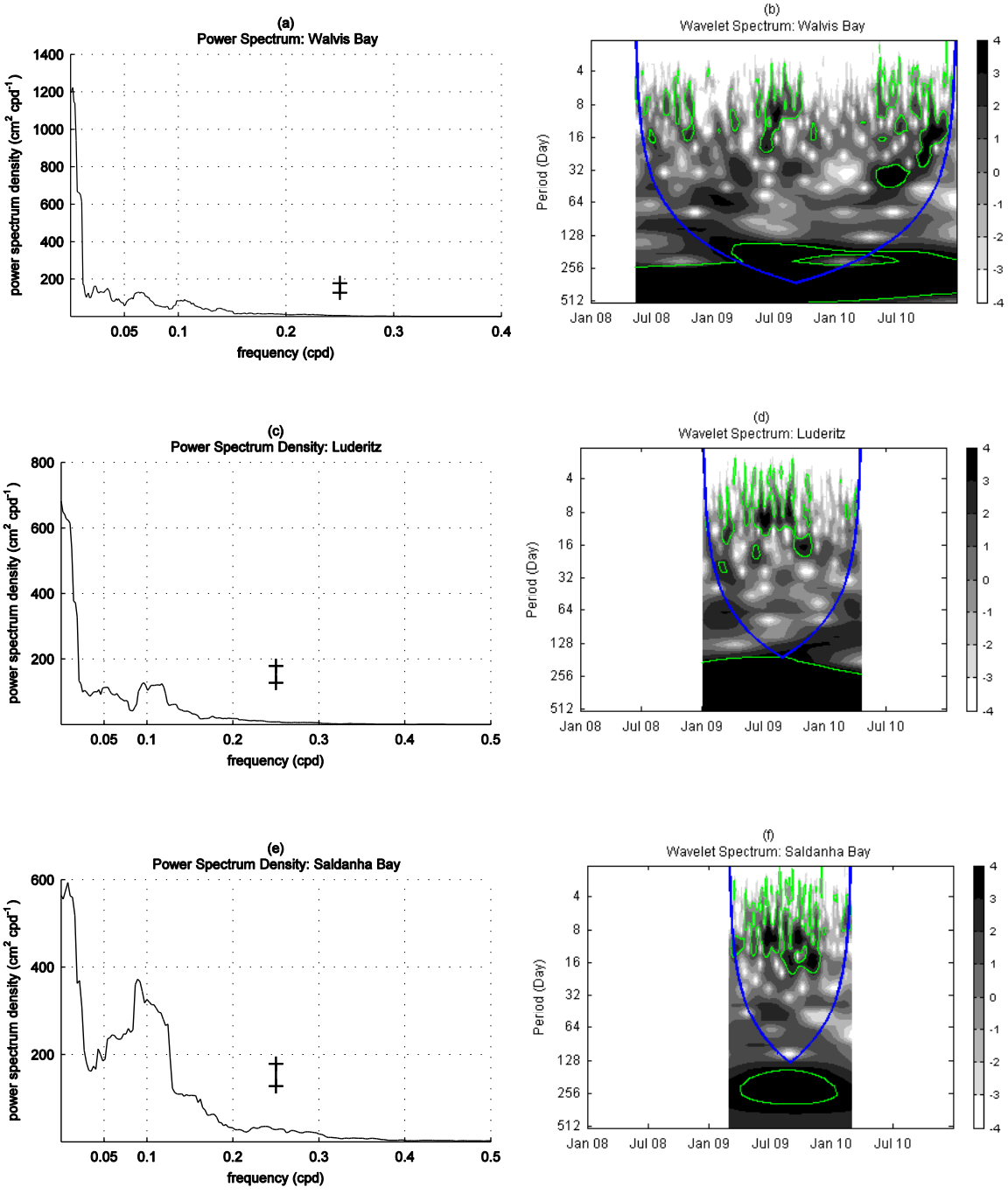

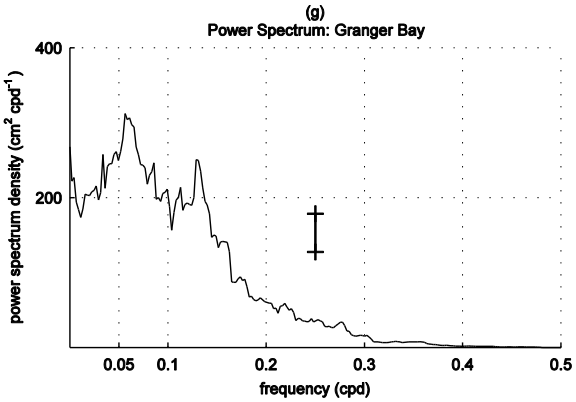
(g)
Power Spectrum: Granger Bay
power spectrum density (cm² cpd⁻¹)
400
200
0.05
0.1
0.2
0.3
0.4
0.5
frequency (cpd)

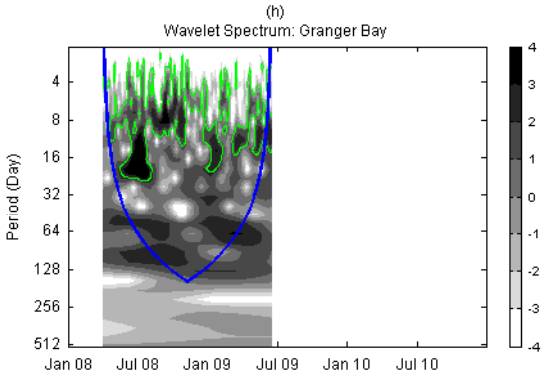
(h)
Wavelet Spectrum: Granger Bay
Period (Day)
4
8
16
32
64
128
256
512
Jan 08
Jul 08
Jan 09
Jul 09
Jan 10
Jul 10
4
3
2
1
0
-1
-2
-3
-4

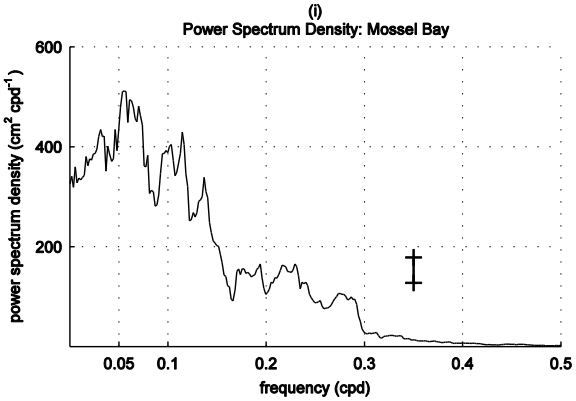
(i)
Power Spectrum Density: Mossel Bay
power spectrum density (cm² cpd⁻¹)
600
400
200
0.05
0.1
0.2
0.3
0.4
0.5
frequency (cpd)

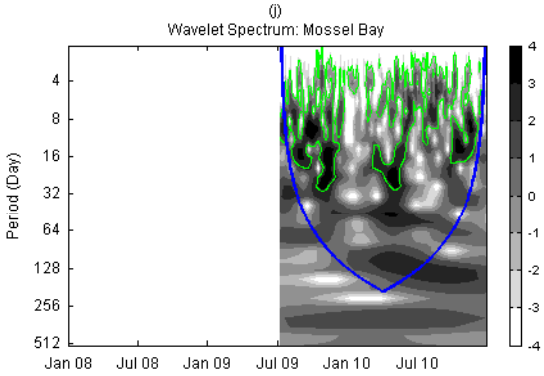
(j)
Wavelet Spectrum: Mossel Bay
Period (Day)
4
8
16
32
64
128
256
512
Jan 08
Jul 08
Jan 09
Jul 09
Jan 10
Jul 10
4
3
2
1
0
-1
-2
-3
-4

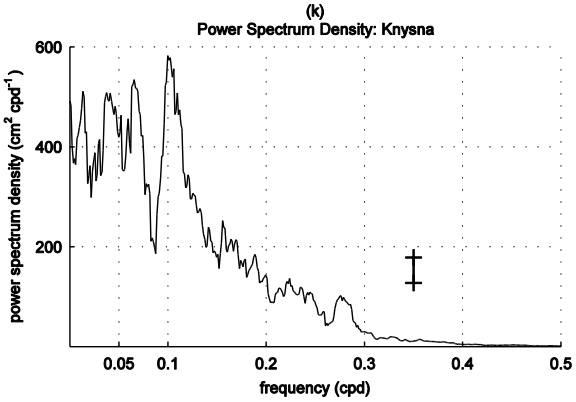
(k)
Power Spectrum Density: Knysna
power spectrum density (cm² cpd⁻¹)
600
400
200
0.05
0.1
0.2
0.3
0.4
0.5
frequency (cpd)

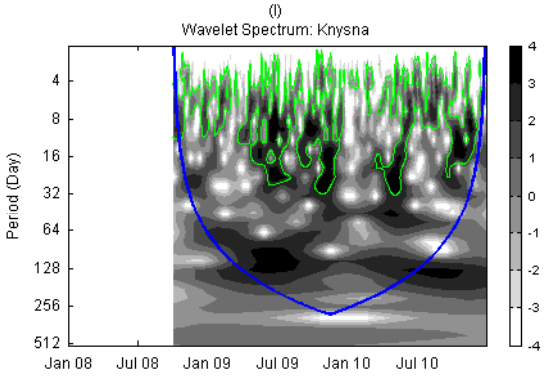
(l)
Wavelet Spectrum: Knysna
Period (Day)
4
8
16
32
64
128
256
512
Jan 08
Jul 08
Jan 09
Jul 09
Jan 10
Jul 10
4
3
2
1
0
-1
-2
-3
-4

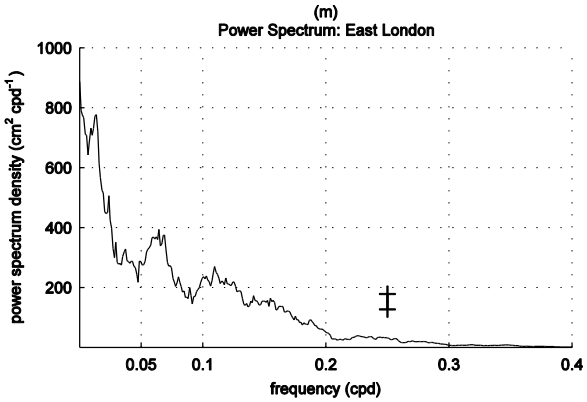
(m)
Power Spectrum: East London
power spectrum density (cm² cpd⁻¹)
1000
800
600
400
200
0.05
0.1
0.2
0.3
0.4
frequency (cpd)

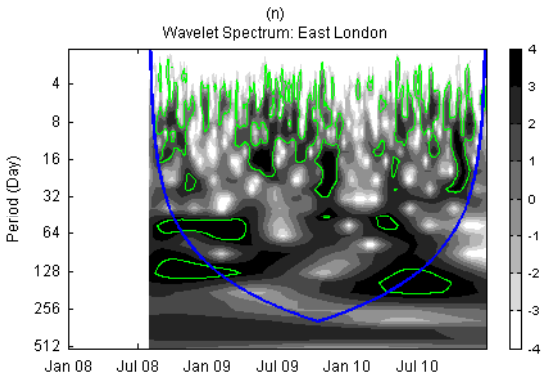
(n)
Wavelet Spectrum: East London
Period (Day)
4
8
16
32
64
128
256
512
Jan 08
Jul 08
Jan 09
Jul 09
Jan 10
Jul 10
4
3
2
1
0
-1
-2
-3
-4

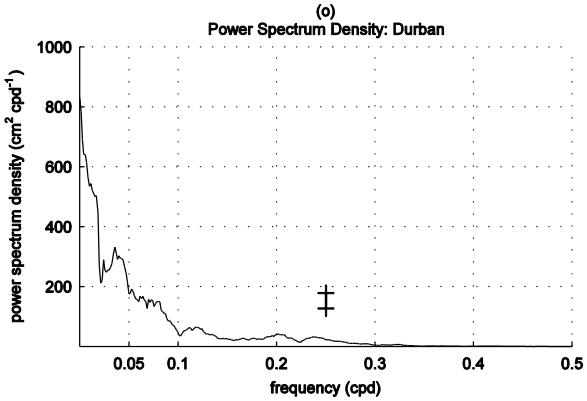
(o)
Power Spectrum Density: Durban
power spectrum density (cm² cpd⁻¹)
1000
800
600
400
200
0.05
0.1
0.2
0.3
0.4
0.5
frequency (cpd)

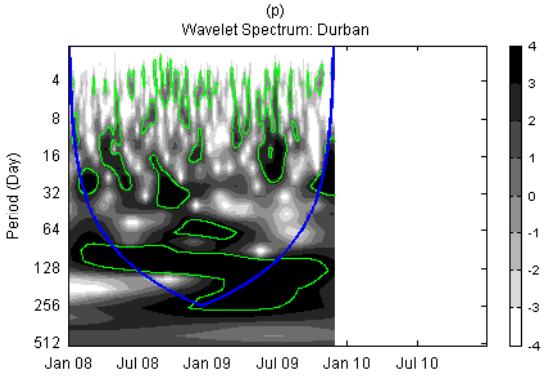
(p)
Wavelet Spectrum: Durban
Period (Day)
4
8
16
32
64
128
256
512
Jan 08
Jul 08
Jan 09
Jul 09
Jan 10
Jul 10
4
3
2
1
0
-1
-2
-3
-4

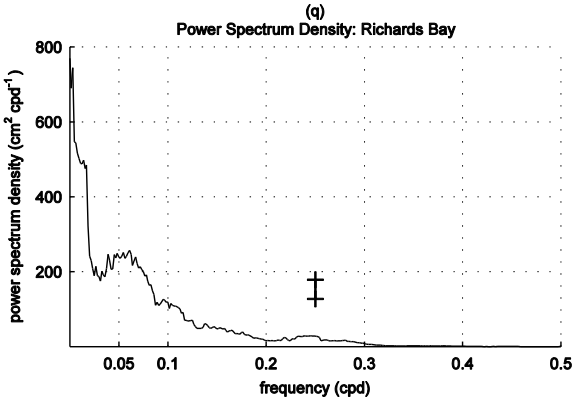
(q)
Power Spectrum Density: Richards Bay
power spectrum density (cm² cpd⁻¹)
800
600
400
200
0.05
0.1
0.2
0.3
0.4
0.5
frequency (cpd)

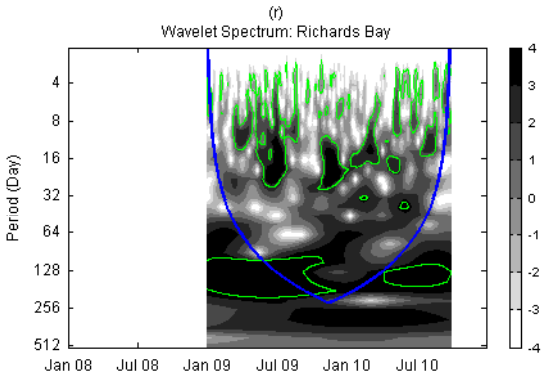
(r)
Wavelet Spectrum: Richards Bay
Period (Day)
4
8
16
32
64
128
256
512
Jan 08
Jul 08
Jan 09
Jul 09
Jan 10
Jul 10
4
3
2
1
0
-1
-2
-3
-4

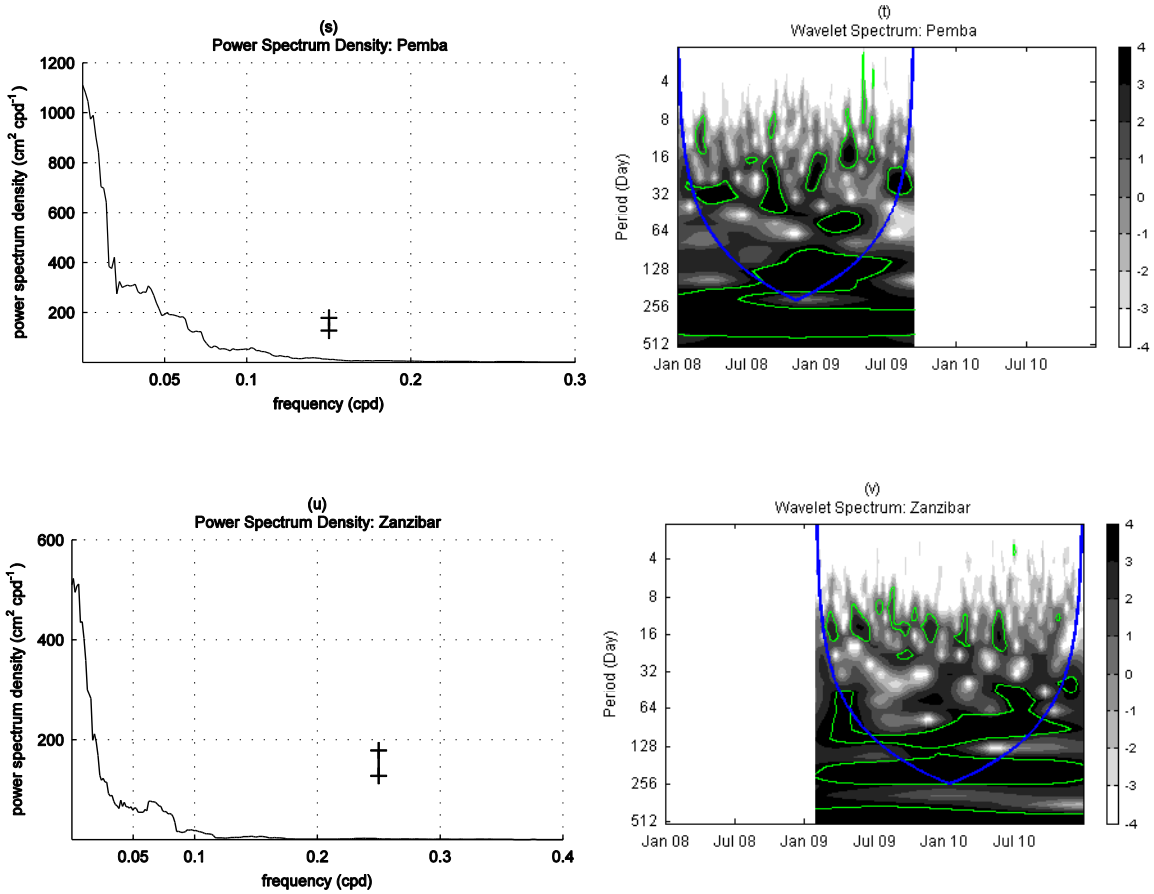


Power spectrum (a), (c), (e), (g), (i), (k), (m), (o), (q), (s) and (u) using the multi-taper method with adaptive weighting for the sea level variability at different tide gauges. 95% confidence (limit) plots are represented. Wavelet power spectrum (b), (d), (f), (h), (j), (l), (n), (p), (r), (t) and (v) for the sea level variability at different tide gauges. Grey shades show the wavelet spectral power (units: base 2 logarithm of sea level variance). The green contour denotes the 95% significance level. Blue line is the cone of influence meaning that anything below is dubious. Each figure is labelled with the name of correspondent tide gauge.

# B. Auxiliary Hovmöller diagrams

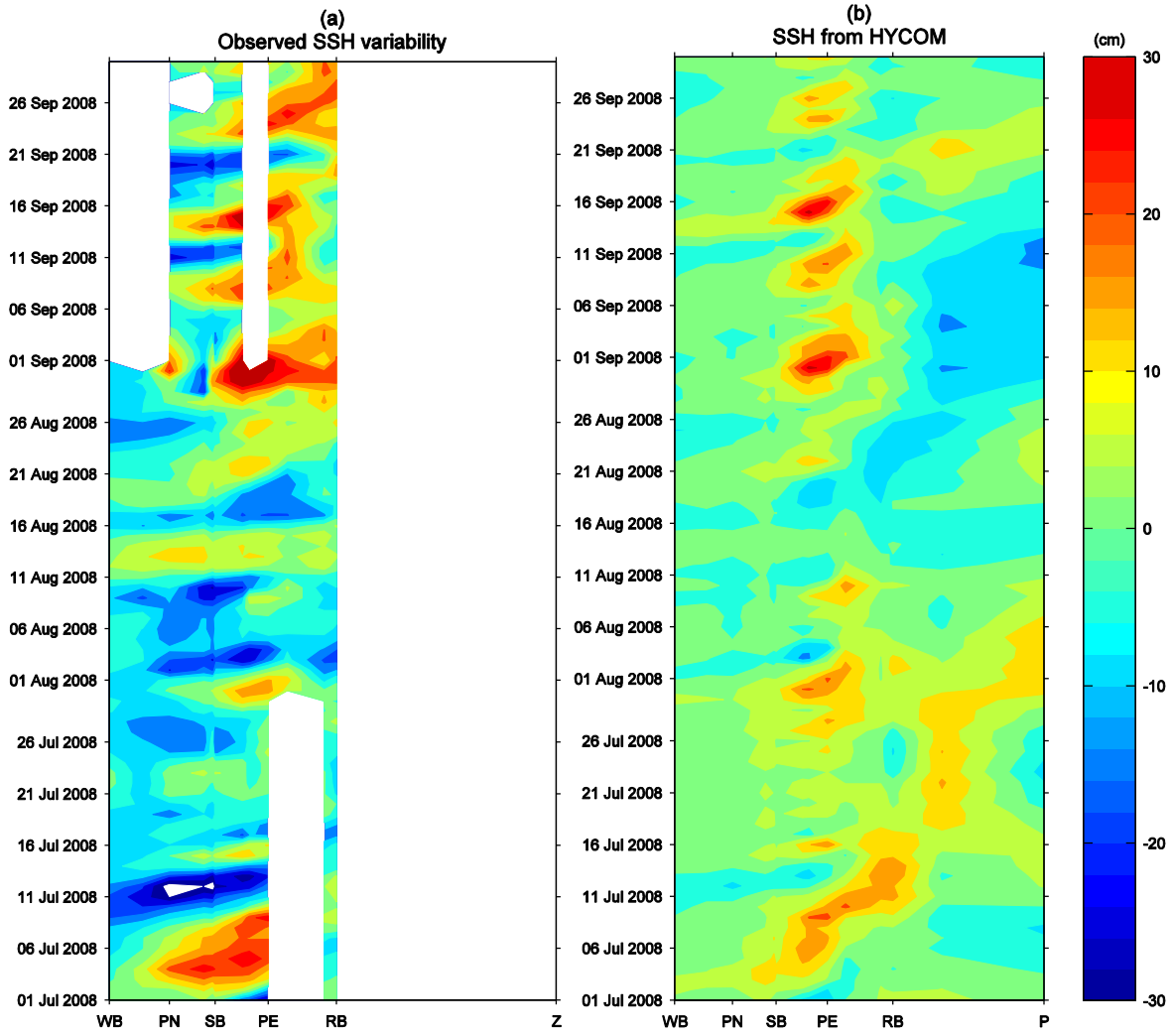

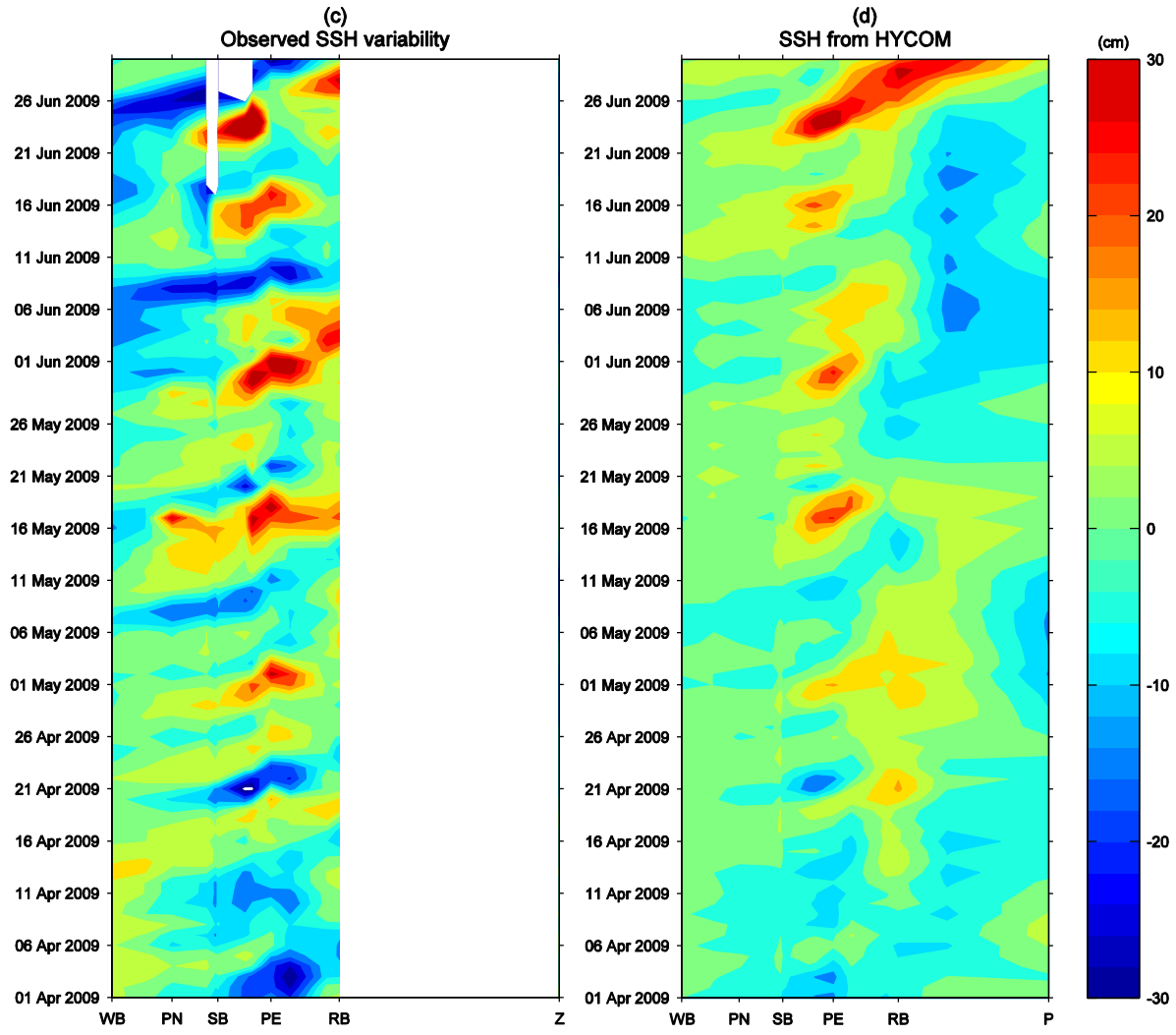
(c)
Observed SSH variability
(d)
SSH from HYCOM
(cm)
30
20
10
0
-10
-20
-30
26 Jun 2009
21 Jun 2009
16 Jun 2009
11 Jun 2009
06 Jun 2009
01 Jun 2009
26 May 2009
21 May 2009
16 May 2009
11 May 2009
06 May 2009
01 May 2009
26 Apr 2009
21 Apr 2009
16 Apr 2009
11 Apr 2009
06 Apr 2009
01 Apr 2009
WB
PN
SB
PE
RB
Z
P

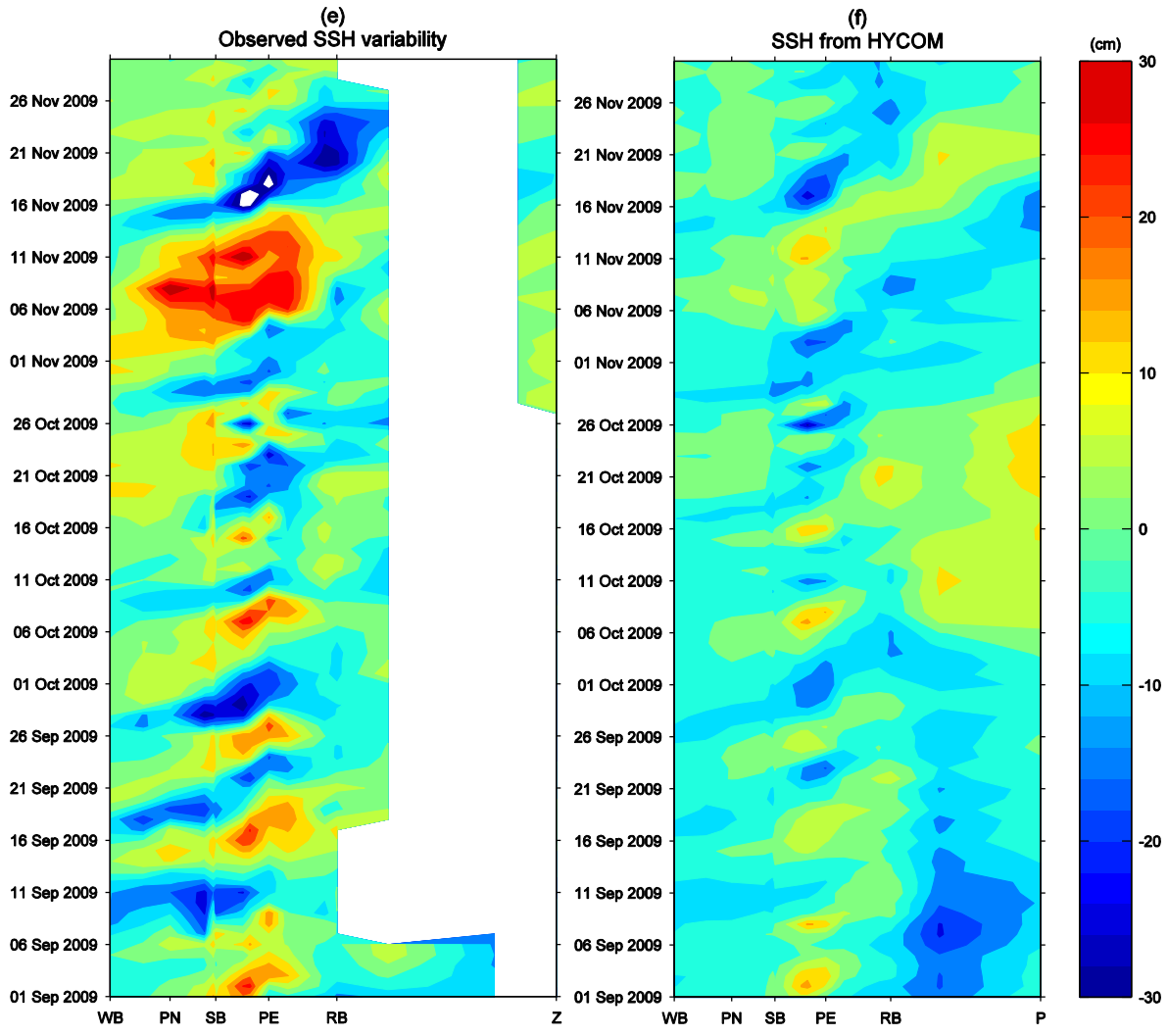
(e)
Observed SSH variability
(f)
SSH from HYCOM
(cm)
30
20
10
0
-10
-20
-30
26 Nov 2009
21 Nov 2009
16 Nov 2009
11 Nov 2009
06 Nov 2009
01 Nov 2009
26 Oct 2009
21 Oct 2009
16 Oct 2009
11 Oct 2009
06 Oct 2009
01 Oct 2009
26 Sep 2009
21 Sep 2009
16 Sep 2009
11 Sep 2009
06 Sep 2009
01 Sep 2009
WB
PN
SB
PE
RB
Z
P

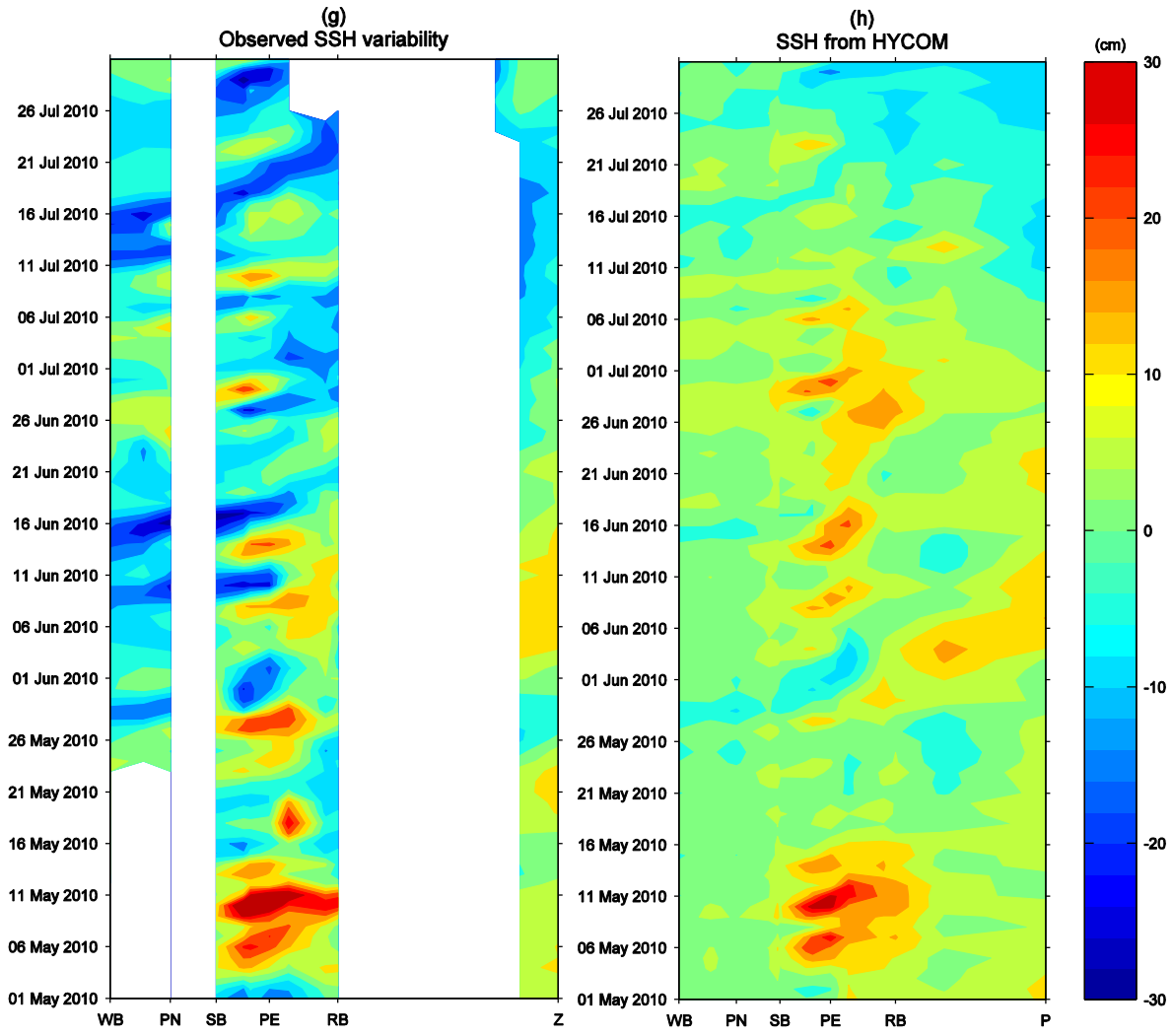
(g)
Observed SSH variability
(h)
SSH from HYCOM
(cm)
30
20
10
0
-10
-20
-30
26 Jul 2010
21 Jul 2010
16 Jul 2010
11 Jul 2010
06 Jul 2010
01 Jul 2010
26 Jun 2010
21 Jun 2010
16 Jun 2010
11 Jun 2010
06 Jun 2010
01 Jun 2010
26 May 2010
21 May 2010
16 May 2010
11 May 2010
06 May 2010
01 May 2010
WB
PN
SB
PE
RB
Z
P

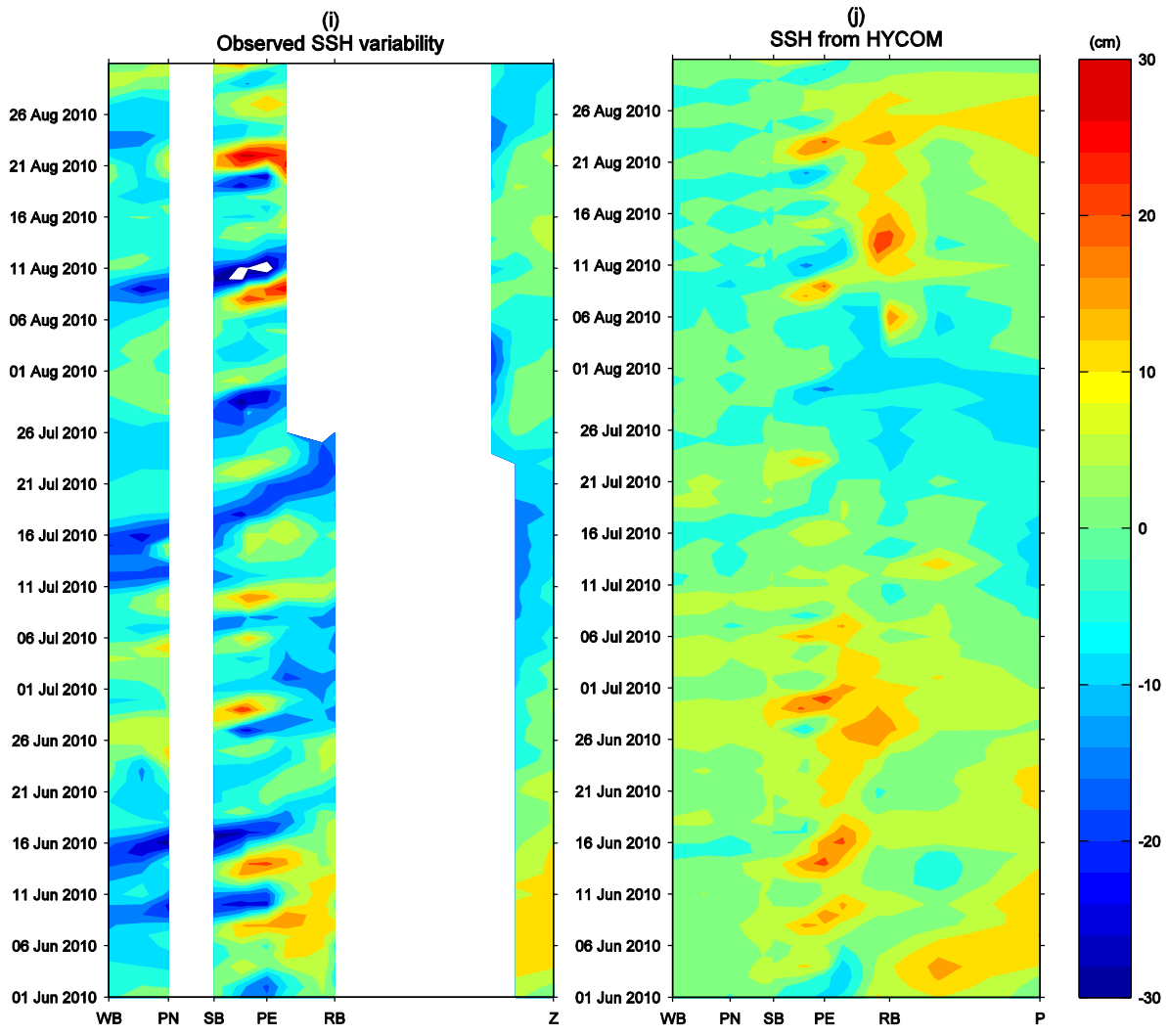
(i)
Observed SSH variability
(j)
SSH from HYCOM
(cm)
30
20
10
0
-10
-20
-30
26 Aug 2010
21 Aug 2010
16 Aug 2010
11 Aug 2010
06 Aug 2010
01 Aug 2010
26 Jul 2010
21 Jul 2010
16 Jul 2010
11 Jul 2010
06 Jul 2010
01 Jul 2010
26 Jun 2010
21 Jun 2010
16 Jun 2010
11 Jun 2010
06 Jun 2010
01 Jun 2010
WB
PN
SB
PE
RB
Z
P

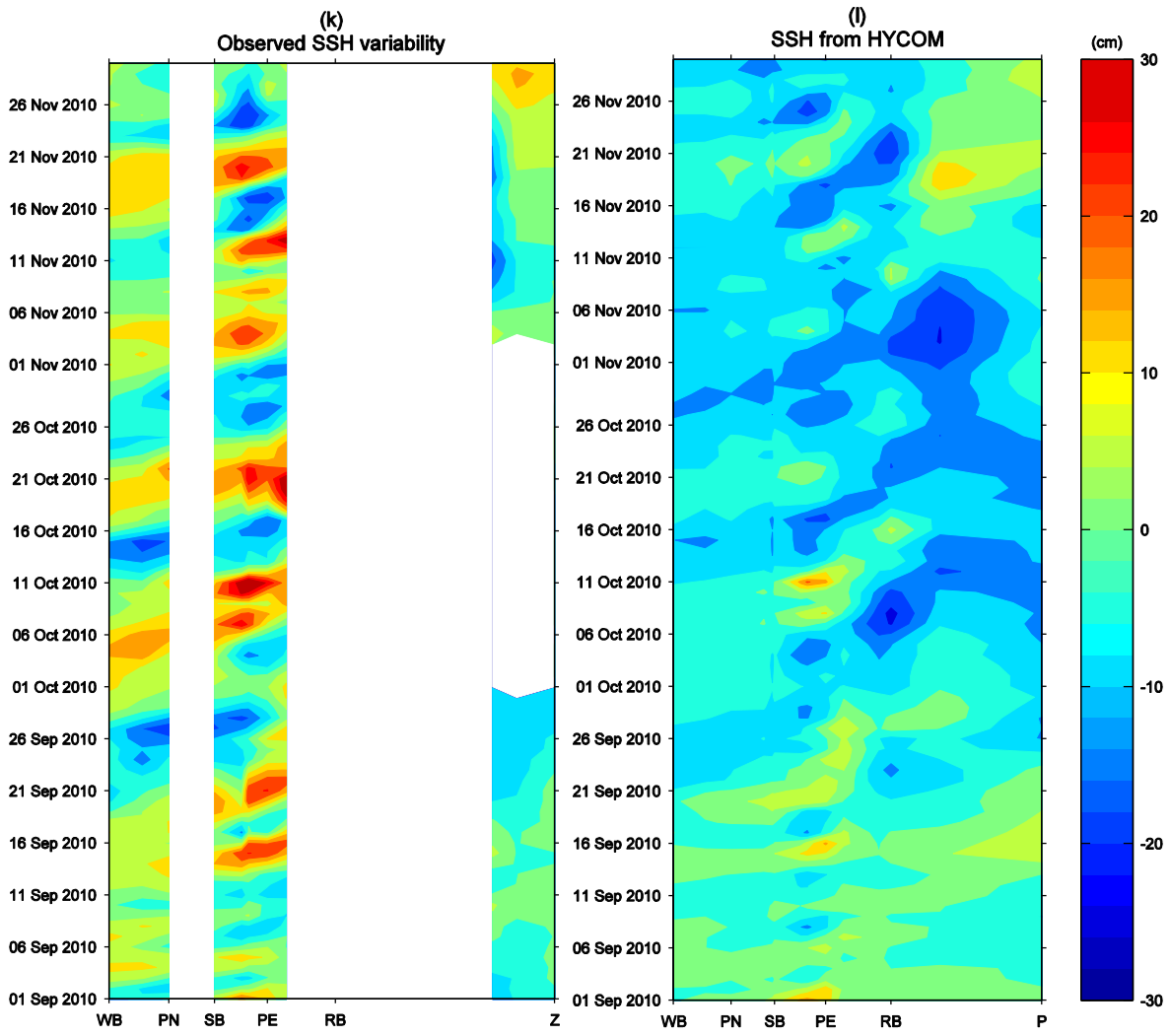


Hovmöller plot for the observed sea level variability (a), (c), (e), (g), (i) and (k), and the sea level variability from HYCOM model (b), (d), (f), (h), (j) and (l) from different periods within the time series. The x-axis represents the distance along the coast from Walvis Bay (WB) to Zanzibar (Z) for the tide gauges, and Pemba (P) for the model output. This spatial difference is due to the HYCOM model domain. White square indicate missing values.

## C. Auxiliary figures of the sequence of daily wind vectors and sea level pressure around Southern Africa

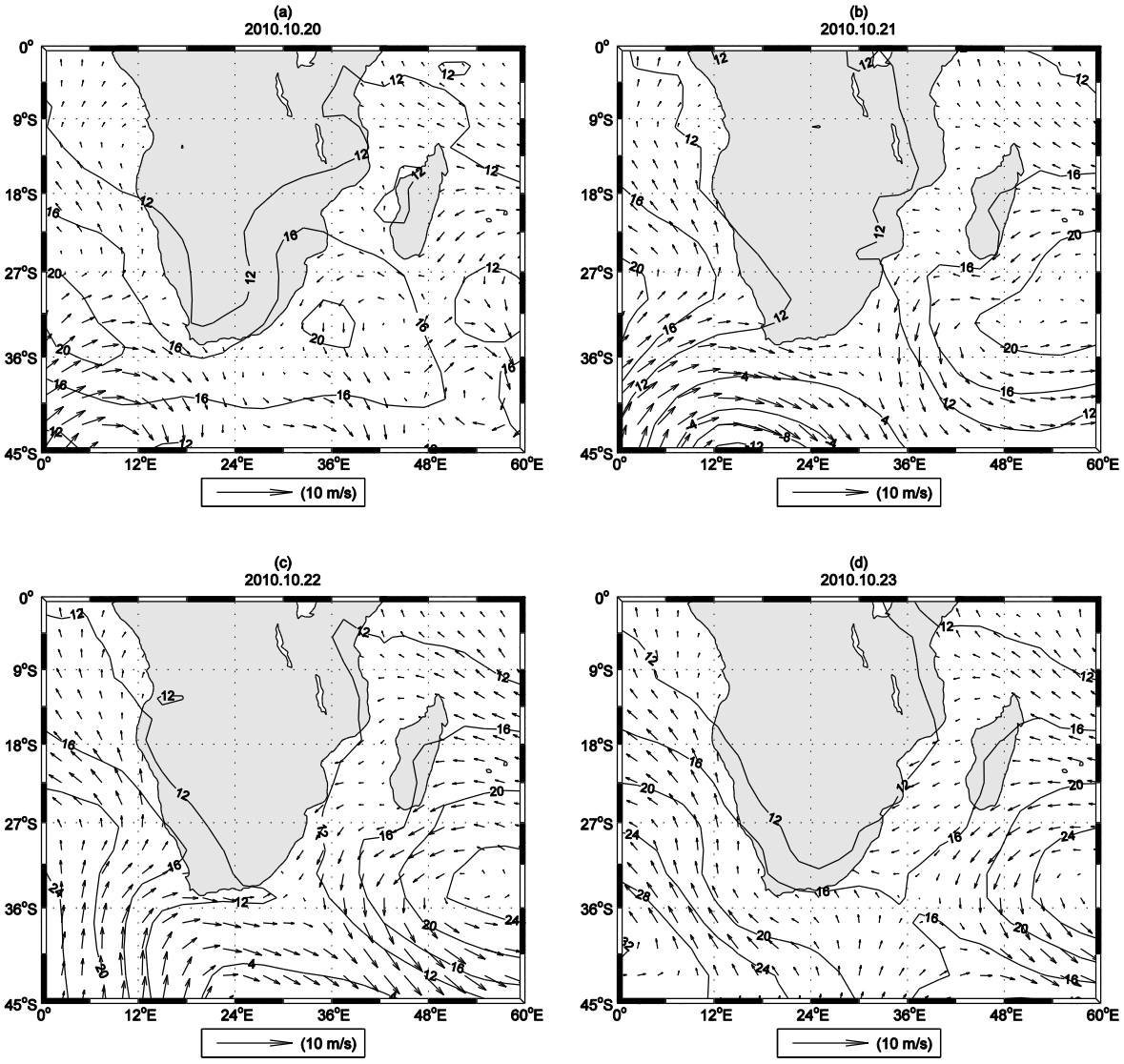

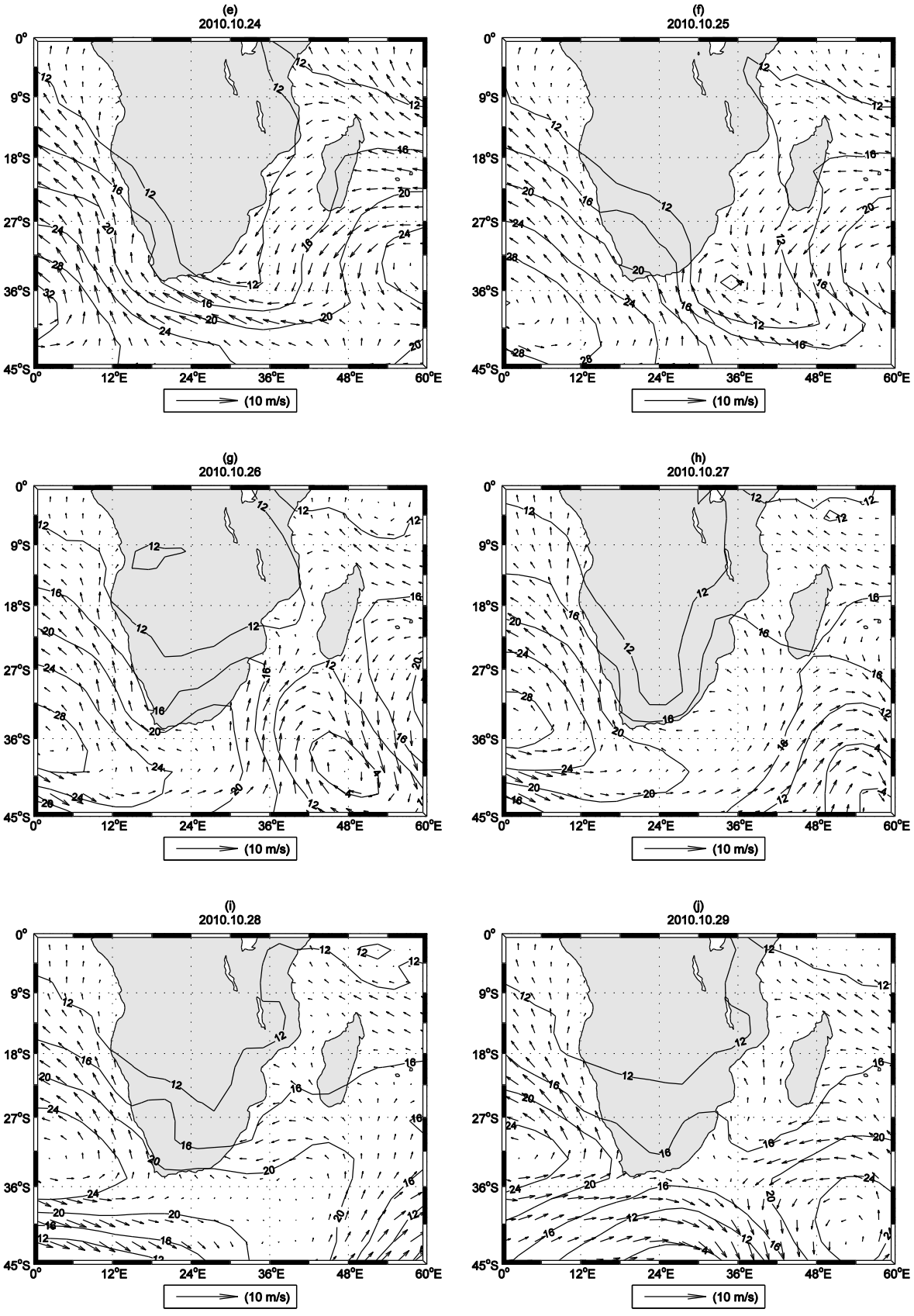
(e)
2010.10.24
(f)
2010.10.25
(g)
2010.10.26
(h)
2010.10.27
(i)
2010.10.28
(j)
2010.10.29
0°
9°S
18°S
27°S
36°S
45°S
0°
12°E
24°E
36°E
48°E
60°E
(10 m/s)

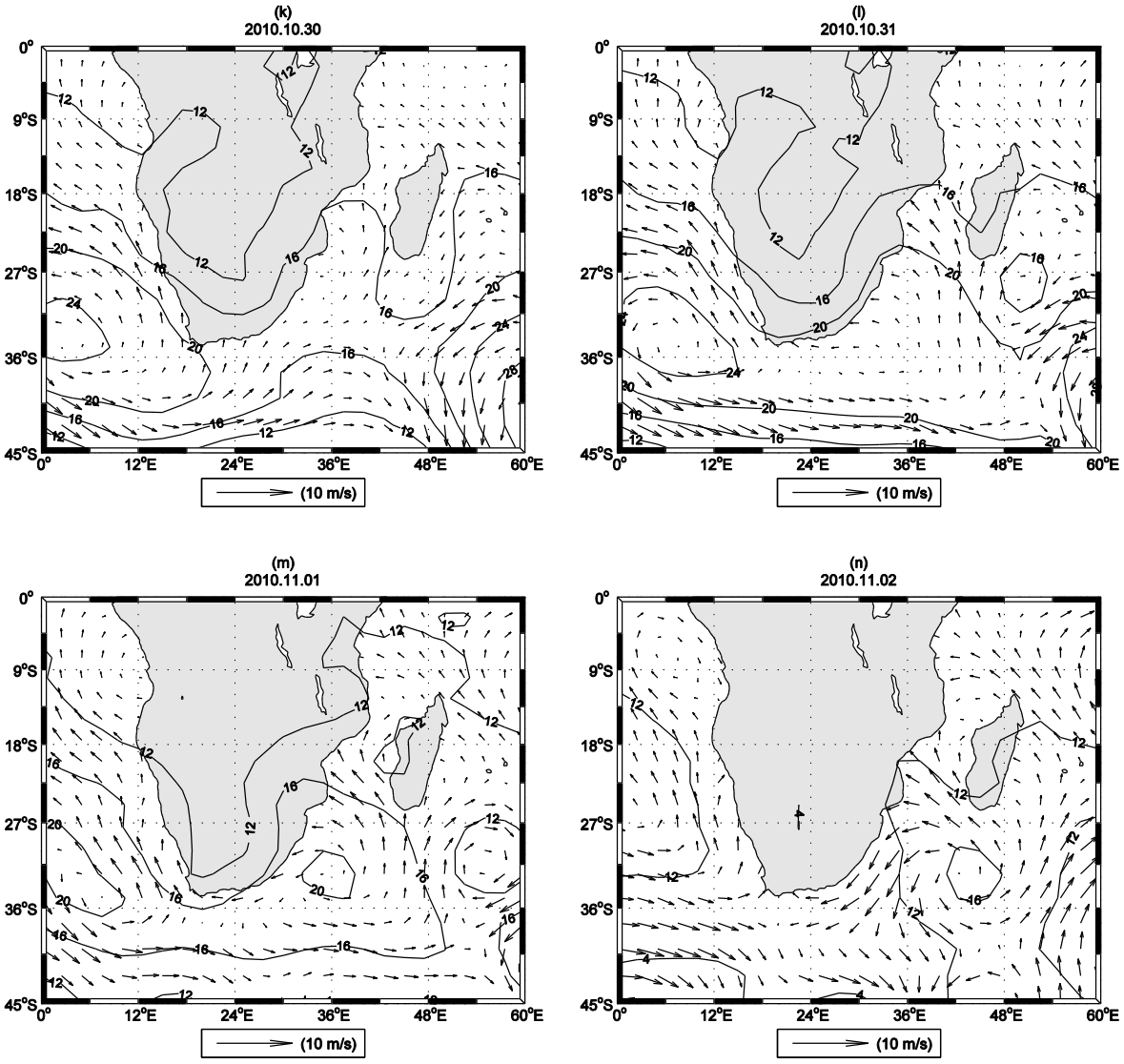


Sequence of daily wind vectors and sea level pressure (contour unit in $10^3$ Pa) around Southern Africa from 20 October to 2 November 2010. For better understanding see also appendix B (k) and (l).